Strål
säkerhets
myndigheten
Swedish Radiation Safety Authority

Authors:
Günther Meinrath
Mike Stenhouse
Paul Brown
Christian Ekberg
Christophe Jégou
Heino Nitsche

Research

2009:33

Workshop on spent fuel performance, radionuclide chemistry and geosphere transport parameters

Lidingö 2008: Overview and evaluation of recent SKB procedures

Report number: 2009:33 **ISSN:** 2000-0456
Available at www.stralsakerhetsmyndigheten.se

Title: Workshop on spent fuel performance, radionuclide chemistry and geosphere transport parameters, Lidingö 2008: Overview and evaluation of recent SKB procedures.
Report number: 2009:33.
Authors: Günther Meinrath, Mike Stenhouse, Paul Brown, Christian Ekberg, Christophe Jégou and Heino Nitsche.
Date: August 2009.

SSM perspective

Background

The safety assessment for disposal of spent nuclear fuel canister in the Swedish bedrock should thoroughly address the time period after a containment failure. Such a failure could be expected as a result of corrosion damage or mechanical failure due to rock movement. This report mainly covers some issues connected to parameters used for radionuclide transport calculations in the areas of spent fuel performance (for fuel in contact with groundwater), radionuclide chemistry, and sorption and geosphere transport parameters. Some examples of topics that are elaborated in some detail include statistical treatment of measurement data (for sorption measurements), handling of uncertainties in speciation calculations, use of triangular distributions in safety assessment and physical processes in connection with spent fuel aging. The results emerged from discussions among international experts at a workshop, Lidingö, Sweden, May 2008.

Purpose of Project

The purpose of this work is providing an overview of ongoing work within the Swedish Nuclear Fuel and Waste Management Co. (SKB), to provide ideas and suggestions for methodology development and to develop review capability within the SSM.

Results

The authors conclude that SKB's treatment of uncertainty in speciation calculations has improved, but that additional efforts in the area of error propagation are recommended. In efforts to condense the scope of utilised thermodynamic databases, the authors recommend that exclusion criteria should be explicitly stated. In the area of sorption, there is a need for more thorough analysis of errors in order to establish uncertainty ranges. The most essential improvements concern dose-limiting nuclides (e.g. Ra-226). Triangular distributions are often featured in SKB safety assessment, but it is not clear that the use of such distributions is based on a firm understanding of its properties. Regarding fuel performance, while safety assessment parameters are supported by measurement data there is still a need for better understanding of the detailed reaction mechanisms and aging effects over very long time-scales.

Future work

In the future, SSM need to develop and extend the knowledge basis for assessment of spent fuel and radionuclide retardation processes. There may also be a need to further expand the capability to conduct independent speciation calculations.

Project Information

Project manager: Bo Strömberg
Project reference: SSM 2008/903
Project number: 200810205, 200810206, and 200810207

Content

1. Introduction

SR-Can covers the containment phase of the KBS-3 barriers as well as the consequences of releases of radionuclides to the rock and eventually the biosphere (after complete containment within the fuel canisters has partially failed). The 2007 review (Stenhouse et al., 2008) and this follow-on report provide a range of review comments concerning parameters related to spent fuel performance as well as radionuclide chemistry and transport. These parameter values are used in the quantification of consequences due to release of radionuclides from potentially leaking canisters. This report does not cover the modelling approaches for quantification of consequences. Such approaches are discussed elsewhere.

Figure 1 gives an overview of the data used for the consequence assessment in SR-Can. Parameter values contained in the red boxes have been (SKI, 2007; Stenhouse et al., 2008) and are addressed by the authors of this report, while parameters with green boxes are addressed in other contexts, e.g. parameters from the hydrology and biosphere assessment that are addressed in e.g. SSM's review of the now-completed site investigations. The groundwater chemistry is addressed to a limited extent as a critical input for the development of a geochemical database and the solubility model used as a basis for estimating radionuclide solubility. In this context, a section is devoted to some relevant properties of Swedish groundwaters.

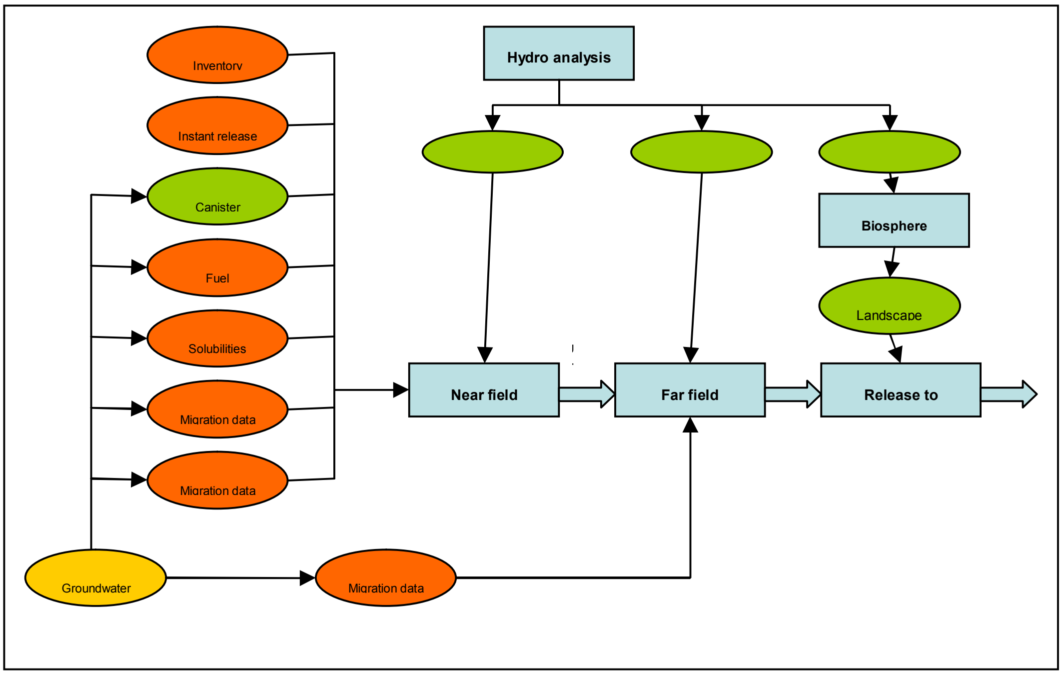

Figure 1: Overview of the data used for the consequence assessment in SR-Can. Parameter values contained in the red boxes are addressed in this report, while the other boxes are addressed in other contexts of the SR-Can review (figure reproduced from SKB SR-Can TR-06-09, page 400).

The work reported here is intended to complement and extend the review findings reported in SKI Reports 2007:17 (SKI, 2007) and 2008:17 (Stenhouse et al., 2008), which cover previous workshops held in 2006 and 2007, respectively, on issues associated with spent fuel dissolution and source term modelling in safety assessment. Topics covered by the review team in these previous reports together with the associated SKB reports include spent fuel performance parameters (Werme et al., 2004, SKB, 2006c), concentration limits in the near field (Duro et al., 2006a) and the supporting thermodynamic database (Duro et al., 2006b), migration parameters in the buffer (Ochs and Talerico, 2004, SKB, 2006d) and far field (Liu et al., 2006, Crawford, 2006, SKB, 2006e).

Additional items reported in SKI Report 2008:17 (Stenhouse et al., 2008) included some details in actinide chemistry and in the 4n+2 decay chain, as well as co-precipitation of radionuclides with major element phases. The decision to focus on the latter was based on the observations in SR-Can, that neglecting co-precipitation of Th-230 may be non-conservative, and that accounting for co-precipitation of Ra-226 with Ba may significantly lower calculated doses. Considering the relatively limited resources available for these reviews, some of the issues have been scrutinised only to a rather limited extent. It is therefore recommended that additional research and review resources continue to be devoted to this area over the next few years.

Uncertainty and sensitivity analysis have framed much of the review discussions over the past three years. An appropriate handling of uncertainties is considered not only important in the context of SR-Site, but also should be apparent in the SKB safety assessment work. In the SSM regulations and guidelines SSM 2008:21 (in 9§ and appendix), it is stated that uncertainties should be discussed and examined in depth when selecting calculation cases, calculation models and parameter values as well as when evaluating calculation results. Thus, a systematic identification and characterisation of the various sources contributing to uncertainty is necessary. SKB's approaches for handling uncertainties related to the relevant safety assessment parameters were discussed in SKI 2008:17 (Stenhouse et al., 2008).

Sensitivity analysis, also required according to the above-mentioned regulation and guidelines, is strongly related to the handling of uncertainties. It is a tool for prioritising the efforts needed in the handling of uncertainties. For example, within the area of spent nuclear fuel and radionuclide chemistry, it is important to ensure the availability of reliable information for those nuclides that contribute the most to calculated dose within various calculation cases.

SSM experts provided a description of alternative/complementary approaches for uncertainty and sensitivity analyses in SKI 2008:17 (Stenhouse et al., 2008) and this treatment is extended in this report to cover, for example, a detailed assessment of the uncertainty associated with the estimation of K_d values.

Section 2 of this report briefly discusses SKB's presentations made at the 2008 Workshop and some highlights from the discussions with SSM and its consultants at the Workshop, Section 3 discusses recent research being carried out in Europe concerning spent fuel dissolution and resultant incorporation of the source term in performance / safety assessment. Section 4 addresses specific aspects of the geochemical database and modelling approach used by SKB to determine solubility-limiting phases for radium and uranium. Section 5 discusses the uncertainties in interpreting groundwater data with particular consideration of the potential effects of microbial systems. Section 6 addresses data reliability from a quality-assurance perspective and examines an internationally-accepted method of evaluating uncertainty, using sorption data as a specific example. Section 7 examines the validity of applying the triangular distribution to account for data variability. Section 8 contains SKB responses to specific questions raised before and during the Workshop on transport properties in the geosphere, specifically concerning measurements of matrix diffusion and sorption-related parameters. Finally, Section 9 provides summary comments.

2. SKB/SKI/SSI workshop

At the SKI-SSI/SKB Workshop in 2008 (May 29), partly in response to previous review comments, SKB and its consultants gave a number of presentations, *viz.*

- Scenario Analysis - Uncertainty and Sensitivity Analysis (Alan Hedin)
- Radionuclide Migration in the Near Field (Patrik Sellin)
- Spent fuel source terms (Kastriot Spahiu)
- Radionuclide solubility limits and thermodynamic data (Lara Duro)
- Radionuclide migration in the Far Field (Jan-Olof Selroos).

While the Workshop itself was not part of formal consultations, the above presentations and the discussions that followed gave SKI's consultants a better understanding of SKB's approach in the selected areas of the SR-Can assessment. Largely as a result of these presentations and the discussions that ensued, some general comments are provided as bullet points below.

- *Scenario analysis*: The main (dose-limiting) scenario involves enhanced corrosion whereby buffer loss (chemical erosion) is the key process. Enhanced corrosion leads to an estimated 9 (out of a total of 6000) canisters failing. As a bounding case, SKB also considered buffer loss immediately, with results similar to the main scenario. While in previous assessments, I-129 was the dominant radionuclide, the current safety assessment results indicated that Ra-226 is now the key (dose-limiting) radionuclide.

- *Radionuclide migration in the near field*: SKB noted that temperature is not a concern with regard to radionuclide release because ambient temperature is reached by the time canisters have failed and radionuclides are released. While Äspö diffusion experiments were not designed for radionuclide transport, they have provided some useful insights into transport in the near field. SKB uses a range of groundwater compositions to allow for mixing waters and bentonite porewater evolution. SKB also noted that the issue of updating the specification for the backfill had still to be resolved, although loss of backfill material does not necessarily lead to higher doses.

- *Spent fuel source terms*: SKB discussed the experimental work that is being carried out to support spent fuel dissolution rates and radionuclide releases for safety assessment calculations, in particular experiments carried out as a function of burnup, with maximum releases observed to occur around 40/45 MWd/kgU. In addition, leaching experiments being carried out by ITU-ENRESA allow comparison of the outer parts of the fuel with the core, with results mainly indicating greater releases from core material (with some expeceptions e.g. Tc). There was detailed discussion about the basis for SKB's instant release fraction (discussed in Section 3).

- *Radionuclide solubility limits and thermodynamic data*: There was significant discussion about error propagation in the context of solubility limits. In this context, the lack of reliable phosphate data, particularly for transuranic elements was also discussed. SKB's current uncertainty propagation is based on variability in groundwater composition rather than error propagation through the thermodynamic database. SKB's objective is to get away from the concept of a 'reference groundwater' and rather accommodate ranges of groundwater component concentrations via multiple (~10,000) realisations. Importantly, SKB noted that a change in solubilities by 2 orders of magnitude either way does not affect assessment results. In addition, if the buffer erosion scenario continues to dominate exposure dose results, solubilities will play a less important role, although under oxidizing conditions, solubility will be important for Np.

- *Radionuclide migration in the far field*: SKB discussed its philosophy for selecting K_d values - generally, with regard to selection of input data, SKB does not want to maximize distribution spread primarily due to a lack of knowledge. Rather the spread should reflect natural variability. Since SR-Can and the sorption values used for assessment calculations, the ongoing laboratory experimental programme was discussed, which is aimed at building a database of site-specific data, combining with a mechanistic model to address any non site-specific data that are used. The new code SDM-Site for the SR-Site assessment describes SKB's current retardation model.

Themes for discussion in the second part of the Workshop included quality assurance (the requirements for the new Data Report are much more stringent) and SKB's general approach to the treatment of uncertainty and the propagation of errors.

SKB emphasized that, although the key (dose-limiting) scenario involves buffer erosion, which is not much affected by solubilities, it is still important to know and address the safety functions of each barrier of the disposal system, with a view to understanding the overall system.

With regard to temperature and the need to consider releases earlier than ~1,000 years when the temperature has returned to ambient, SKB observed that one of the conclusions from the SR-Can assessment was that earlier releases are not justified. Even if canister failure occurs earlier, a long time is needed before the solubility limit is achieved, because of the slow dissolution rate for spent fuel.

Coprecipitation of Ra-226 with barium was discussed with interest in this process shown by both SKB and SSM. SKB's experimental programme involving coprecipitation in barite and strontianite and the preliminary results indicate that coprecipitation does occur. The likelihood exists, therefore, that Ra-Ba coprecipitation will be included in the SR-Site assessment.

Many of the topics discussed at the Workshop are developed further in the following sections.

3 Spent Fuel Dissolution – Current Issues and Recent Research

3.1 Instant Release Fraction

The definition of the instant release inventories remains one of the most controversial subjects in recent years at an international level. Two main options can be considered to define the instant release inventories:

- One option is to define the instant release inventories and their uncertainties based on parameters related to reactor irradiation conditions (LP, FGR, etc.) as well as experimental data (initial characterization and leach testing) obtained on fuel after a few years of cooling.
- The second approach seeks to integrate the uncertainties on the mechanisms of long-term fuel evolution; this implies redefining the instant release inventories to allow for contributions that are not currently taken into account in the preliminary approximation, and tends to increase the source term.

The latter approach attempts to redefine the instant release inventory by allowing for uncertainties in the possible long-term fuel evolution mechanisms (radionuclide migration towards the “free space” under alpha self-irradiation, stability of the grain boundaries and closed porosity, increased surface area, etc.). Such an approach implies that an inventory not initially subject to instant release (i.e. not directly accessible to water) in the fuel could become so over the long term when water comes into contact with the waste package after several thousand years in a closed system.

Clearly, in this context, the definition of the instant release inventories will depend to a large extent on the state of knowledge and understanding of the mechanisms capable of modifying these inventories. Leaching data obtained with un-aged fuel will be difficult to extrapolate over the long term if these mechanisms are of significant magnitude.

The risk with this approach would be to propose instant release values that are too unfavourable and overly-conservative. Such an approach should therefore be considered as incremental with the current state of knowledge, but appears to be highly appropriate for investigating the long-term behaviour of a waste package and suitable for the time scales involved.

With regard to the instant release fraction, two processes have been the subject of several studies in recent years. One is the diffusion, enhanced by alpha self-irradiation, of radionuclides from the UO_2 matrix toward the exterior of the grains. The other concerns the long-term stability of the grain boundaries under the effects of helium accumulation and irradiation damage in the ceramic material. Both processes would be capable of modifying the instant release inventories over time.

3.1.1 Diffusion process in spent fuel – new data and conclusions

Most of the theoretical approaches developed to date to estimate diffusion accelerated by alpha self-irradiation yield low diffusion coefficients, although when the models are applied to in-reactor operation they are unable to account for the experimental data either.

Heavy ion bombardment of implanted UO_2 disks has been used to simulate the effects of alpha self-irradiation on iodine mobility (Saidy et al., 2007);

- The UO_2 disks were implanted with iodine (I-127) of 800 keV at fluences of $10^{11}$and 10^{12} at/cm^2.
- Samples were irradiated under various conditions in order to simulate the mobility of atoms due to (i) ballistic collisions created by recoil atoms (equivalent to irradiation damage similar to the ballistic damage in spent fuel after 10,000 years), or (ii) electronic excitation induced by alpha particles.
- Iodine profiles were measured by SIMS before and after irradiation.

The results from these experiments indicate no measurable displacement (<50 nm) of iodine, which implies a reduction in diffusion coefficient from around 10^{-27} to 10^{-29} m^2/s. The diffusion coefficient, *D*, is proportional to the volume alpha activity, A_α,

$$D = 2 \times 10^{-45} A_\alpha$$

Such a diffusion coefficient yields a maximum diffusion distance of ~10 nm in 10,000 years.

With regard to activation products, Pipon et al. (2007), on the basis of experiments performed on implanted UO_2, demonstrated that thermal diffusion of chlorine in UO_2 is higher than for I and Cs. The same behaviour is observed under irradiation. Due to uncertainties concerning the behaviour of activation products, however, the contribution of the diffusion process to the instant release inventories of Cl-36 and C-14 is based on the upper estimate of the diffusion coefficient value, *i.e.*

$$D = 2 \times 10^{-41} A_\alpha$$

3.1.2 Fate of helium in spent fuel rods

The variation in fuel surface area over time is related to the formation of gases - notably helium under alpha decay. The importance of gas formation over the long term has not been satisfactorily quantified to date, especially in high burn-up fuel and in the rim for intermediate burn-up levels.

The fate of helium depends on its diffusion and solubility properties, which have been relatively well studied in UO_2, indicating low diffusion lengths and relatively low He solubility compared with He production in spent fuel. Recent experiments (Pipon et al., 2007) indicate the precipitation of helium in new intra-granular bubbles and in pre-existing intra-granular fission gas bubbles prior to helium release into grain boundaries. Thus, based on theoretical models and experiments simulating the effects of alpha decays on the atom mobility in spent fuel, combined with theoretical models, the release of fission products to grain boundaries should not be significant even on the long term.

Assuming a uniform distribution of pores with pore size ranging between 0.5 μm and 2.5 μm in accordance with literature data and a total porosity of 15% in the RIM, the local quantity of helium produced after 10,000 years of disposal should not be sufficient to reach the critical value leading to propagation of cracks in the rim region.

3.2 Matrix Alteration

Two mechanisms may govern the immediate or long-term alteration of the spent fuel matrix in a repository environment:

- Oxidising dissolution under the effect of radiolysis;
- Uranium dissolution controlled by solubility.

Recent results (Poinssot et al., 2005) demonstrated that radiolytic dissolution is the governing alteration process above a critical activity threshold (18-33 MBq/g).

3.2.1 Influence of hydrogen

Experiments in the presence of H_2 indicate:

- Inhibition of fuel dissolution, resulting in almost immeasurable alteration rates.
- Activation of H_2 is assumed to be related to the UO_2 surface, epsilon metallic phases, and/or some other catalyst. However, the mechanism has yet to be understood.

If H_2 activation is confirmed, H_2 contributes to the global redox balance. However, the influence of the redox buffer capacity of the environment seems to be high enough to counteract the radiolysis effect. In this sense, H_2 inhibition may not be the primary process.

Thus, the mechanism responsible for the inhibiting effect of H_2 is still undetermined (possibly consumption of oxidants, an activation mechanism, or related to the UO_2 surface and metallic phases) and therefore requires additional studies to substantiate its inclusion in PA calculations. Allowing for hydrogen in PA calculations also requires that hydrogen be present in sufficient quantities at the reaction interface.

The acquisition of kinetic data on the effects of low-flux alpha radiolysis constitutes another pertinent area of investigation in addition to hydrogen studies. A long-term alteration rate at low flux would probably consolidate these low alteration rates irrespective of the presence or absence of hydrogen. The hydrogen effect could then be considered an additional safety factor during the phase in which it is produced by canister corrosion.

3.2.2 Conclusions regarding spent fuel matrix alteration

Given the present state of knowledge, the proposed release fractions – between 10^{-6} and 10^{-8} per year for the spent fuel matrix after disposal - are reasonable and realistic. Their robustness is supported by the fact that they were determined via examination of a broad and exhaustive experimental data set, resulting in a final variation over two orders of magnitude.

The absence of any explicit time-dependence of the alteration rate is worth noting, and in fact reflects the absence of a true, relatively general kinetic law of alteration capable of integrating key environmental parameters (oxidant scavengers, etc.) and variations over time (oxidant concentrations, surface area, etc.).

3.2.3 General considerations on the Rapid Release Fraction used for PA

The fractional release rate (FRR) can be expressed in terms of the following equation:

$$FRR = R\, S \,/\, m_{matrix} \text{ (per year)}$$

where R is the intrinsic parameter (alteration rate, g m^{-2} yr^{-1}), S is reactive surface area (m^2) and m_{matrix} is the mass of the matrix (g), i.e., the release fraction is related to a reactive surface area.

Even if advances are possible on improving the value of the intrinsic parameter R according to alteration conditions (inhibiting effect of hydrogen, decreasing concentration of oxidizing agents over time, etc.), to what extent are these imporvements not likely to be called into question by a variation in the reactive surface area of the spent fuel on a repository time scale?

It is clear that the low burnup values of the Swedish fuel tend to be favourable and should limit the problem of microcracking at the grain boundaries due to helium accumulation. Moreover, processes may also lead to a reduction in the reactive surface area (precipitation of secondary phases, diminishing reaction site density, etc.) as shown by several authors. However, it remains difficult to assign a weighting to each of these processes over the long term.

3.3 Overall Conclusions on Spent Fuel Source Term

With regard to the IRF, while a robust model exists for quantifying this release fraction, improvements are needed to decrease the current uncertainty and associated conservatism – measurement on fresh fuels; assess the evolution of grain boundaries – can they open with time?

With regard to the matrix, radiolytic dissolution is expected to be a significant early process, but the activity threshold needs to be assessed better. For PA, the hydrogen influence on radiolysis may be of second order – the redox buffer capacity of the environment may sufficiently hinder the radiolysis. Solubility-controlled dissolution needs to be studied, in particular, the influence of the U(IV) secondary phases.

4. Geochemical Database and Solubility Model

4.1 Modelling Approach

The modelling approach adopted by SKB involved a multiple step process for each groundwater scenario investigated. The following steps have been identified (this is based on the Excel spreadsheets provided to SKI with filenames "*simple functions.xls*" and "*simple functions & uncertainty.xls"):*

1. The total concentration of each major component in a particular groundwater scenario is input into the model (for the scenario data see Table 3-1 in Duro et al. [2006a]). However, it would appear from the spreadsheets provided that SKB have been somewhat selective in the major ions they have included in the model. For example, neither Mg nor K is included in the model calculations. Physicochemical parameters are also input into the model.
2. The free concentrations of each of the major components are calculated from their combined respective total concentrations and a defined set of stability constants for complexes that may form between the cations and anions (plus protons and hydroxide ions) in a particular groundwater scenario. This is by necessity an iterative procedure and also takes into account the ionic strength of the groundwater under consideration.
3. The solubility limit for each radionuclide is then determined separately using both the aqueous speciation of the radionuclide under consideration and the likely mineral phases that could control its solubility.
4. When considering the solubility of a particular radionuclide with respect to a given mineral phase, the calculation will typically consider the free concentration of the radionuclide. The free concentration must then be adjusted to the concentration limit by considering the speciation of the radionuclide i.e. the total concentration of the radionuclide is determined from its free concentration on the basis of the free concentration being controlled by a particular mineral phase. In essence, this is the reverse of the calculations performed in steps 1 and 2 above. Again, SKB seems to have been somewhat selective in the choice of potential aqueous species that may form for a given radionuclide. For example, neither UO_2OH^+ nor $(UO_2)_2(OH)_2^{2+}$ have been considered as aqueous species in the estimation of minerals that control the concentration of uranium. The choice of species, however, may have been dependent on expert judgement since, for example, with the two uranium species identified above, it may have been argued that, under the physicochemical conditions identified in the various groundwater scenarios, neither of the two species would be considered to be important.
5. For each radionuclide a range of mineral phases are considered and the one that leads to the lowest predicted solubility for the radionu-

clide in question is deemed to be the solubility limiting phase and the radionuclide concentration predicted is the concentration limit.

6. Uncertainty calculations were then undertaken utilising the defined errors associated with each stability constant and solubility product.

An assessment of the uncertainty analysis performed by SKB has been previously documented (Stenhouse et al., 2008). There are, however, factors in the modelling methodology adopted by SKB that may lead to potential additional numerical uncertainties. These factors and the potential uncertainties they may introduce were not discussed in Stenhouse et al. (2008).

It is not clear why SKB have been selective in choosing the major ions to be included in the model. The species included in the spreadsheets identified above are consistent with those in the PHREEQC database (*solub_05_sent.dat*) also provided by SKB. The exclusion of Mg and K may have a considerable impact on the magnitude of the free anion concentrations (in particular, sulphate) since these cations are important in at least one of the modelled groundwater scenarios. Magnesium has the third highest cation concentration in the reference groundwater and K the highest concentration in the buffer-equilibrated water. For the reference groundwater scenario, for example, the modelling conducted by SKB indicates that aqueous complexes account for about 33% of the total sulphate concentration, predominantly $CaSO_4$(aq) and $NaSO_4^+$. If Mg had been considered, aqueous species would account for about 45% of the total sulphate concentration, with $MgSO_4$(aq) accounting for the additional 12%. The effect of this is to decrease the free sulphate concentration, and consequently, increase the calculated solubility limit of any radionuclide controlled by sulphate minerals, such as Sr and Ra.

The separation of the speciation calculation for the major ions from the radionuclide solubility limit calculation may at first glance seem reasonable since the majority of radionuclides are controlled at relatively low concentrations that are unlikely to have a significant effect on groundwater conditions. In reality, this may be illusory since the amount of any radionuclide precipitate formed may also have an impact on the aqueous geochemistry, and hence, the groundwater conditions. For example, the precipitation of oxide and/or hydroxide phases will release protons into solution, the magnitude of which depends on the amount of these phases that precipitate but protons so released could potentially modify the pH of the groundwater. Similarly, the precipitation of sulphate phases, such as those of Sr and Ba (produced from the decay of radioactive Cs), will lead to a decrease in the free concentration of sulphate, again the magnitude being dependent on the amount of the sulphate phases that precipitate. This, in turn, may lead to an increase in the concentration of other radionuclides, such as Ra, that are also controlled by sulphate phases. Further, radionuclides that have a relatively large concentration limit may impact on the groundwater conditions by changing such parameters as the ionic strength or the free concentrations of the major ions. It would appear, therefore, that the separation of the modelling into two steps may add considerable uncertainty to the calculated solubility limits for a number of, if not all, radionuclides.

The situation would appear to be further exacerbated by the exclusion of some important species for a number of radionuclides. It is inappropriate to omit such species in speciation calculations even if it is perceived that they will not be important under the conditions modelled. If any particular species is unimportant the speciation modelling will indicate this fact but not including a species in a model prevents the species from *becoming important if the modelled conditions change.* Some examples of missing species include:

- UO_2OH^+ and $(UO_2)_2(OH)_2^{2+}$. Although it is possible that both of these species may be relatively unimportant in the scenarios modelled, they may become important if the groundwater conditions change. Certainly, the latter species $(UO_2)_2(OH)_2^{2+}$ will be more important than the other dimeric species that has been considered in the model i.e. $(UO_2)_2CO_3(OH)_3^-$. Further, it is also not clear why polymeric hydrolysis species have not been considered for either Np(VI) or Pu(VI). The solubility of Np and Pu, similar to that of U, is controlled by their respective tetravalent oxide / hydroxide, and polymeric U(VI) species are considered for U.
- Sulphate species of Ni, U, Np and Zr. Data for each of these radionuclides are available in their respective NEA thermochemistry reviews. Again, many of these complexes may be relatively unimportant but the presence of those of Ni, for example, may further reduce the free sulphate concentration.
- No consideration is given whatsoever to the speciation of stable decay products such as Ba, which may also affect groundwater conditions, and therefore, the concentration limits for various radionuclides.
- Various carbonate species for U, Np and Pu. It is not clear how the species have been selected based on the available data given in various literature reviews since there appears to be no obvious pattern to the selection process for the species chosen for the three radionuclides.

Other examples may occur. The methodology used by SKB for the selection of both elements and their respective species is unclear. Although it may be based on expert judgement this is neither stated explicitly nor is it appropriate. The apparent exclusion of data will undoubtedly lead to increased uncertainty with respect to the concentration limits assigned. This will be further exacerbated by the separation of the modelling into the two distinct steps since the likelihood exists that certain radionuclides that have an elevated solubility limit will affect groundwater conditions such as ionic strength, major ion concentrations, and potentially, pH and Eh. It is surely a requirement that the solubility estimates use as an initial input the estimated release rates of radionuclides from canisters under various scenarios and flow rates of the groundwater. Given that the release rate of one radionuclide and its associated concentration could affect the solubility of another, it would appear that, at best, solubility calculations should be undertaken using all radionuclides together (plus their stable decay products) or, at least, the uncertainties associated with the solubility limit calculations should be increased to take account of these factors.

4.2 Radium Database and Solubility Limits

Only a very small number of species / mineral phases have been considered in the solubility modelling of Ra conducted by SKB (Duro et al., 2006a): four aqueous species ($RaOH^+$, $RaCl^+$, $RaSO_4(aq)$ and $RaCO_3(aq)$) and two solid components ($RaSO_4(s)$ and $RaCO_3(s)$). This is not surprising since the aqueous chemistry of radium rarely has been studied and it is unlikely that additional data are available in the literature. The only mechanisms that could be utilised to increase the database for radium would be to use either linear free energy relationships or theoretical models that predict stability constants. The use of either of these mechanisms is not recommended because it is improbable that the overall conclusion reached by Duro et al. (2006a) would change; that is, that the dominant species of radium present in each of the groundwater scenarios considered is Ra^{2+}.

One of the scenarios modelled contains phosphate in the groundwater at a relatively high concentration (0.0323 mmol dm^{-3}). As such, it is suggested that the SKB database for Ra be supplemented by the inclusion of some phosphate data. The presence of phosphate in such scenarios may control the Ra concentration. The solubility of $RaHPO_4$, the phosphate phase that will most likely control Ra solubility at circumneutral pH, has been estimated by Jeffree et al. (1993) using an electrostatic method. The value obtained for log K_s was -7.55 (the values used for the experimentally measured solubilities of Mg, Ca, Sr and Ba hydrogen phosphate [log K_s] were -5.735, -6.583, -6.96 and -7.46, respectively [Jeffree et al., 1993]).

The results of SKB (Duro et al., 2006a) indicate that $RaSO_4$ is the phase that controls Ra solubility in all four groundwater scenarios modelled and that the maximum aqueous concentration was predicted to be about 10^{-7} mol dm^{-3} for all four scenarios. In fact, both SKB (Duro et al., 2006a) and SKI reviewers (Stenhouse et al., 2008) have suggested that the presence of Ra-Ba-Sr coprecipitates (the sulphate minerals barite [$BaSO_4$] and celestite [$SrSO_4$] control the aqueous concentrations of Ba and Sr, respectively) is likely to decrease the Ra concentration by several orders of magnitude. Therefore, the use of $RaSO_4$ to control Ra solubility is likely to be conservative. However, there are potentially some instances where these sulphate minerals may not fully control the concentrations of Sr, Ba and Ra. These instances include reducing groundwater where sulphate may be reduced to sulphide (Stenhouse et al., 2008) or where aqueous metal concentrations that form either sulphate complexes or mineral phases exceed the sulphate concentration (for example, the predicted maximum concentration of Sr is approximately 10% of the sulphate concentration of the reference groundwater – such analysis does not take into account other metal ions that may also bind with sulphate, as discussed above).

4.3 Uranium Database and Solubility Limits

There are a number of concerns relating to the database created for U and the way that it has been used to determine the solubility limit for U. These concerns include:

- The calculation for the solubility limit of U undertaken by SKB is incorrect. The free U concentration can be determined from the solubility constant of the controlling phase and the determined concentrations of the major ions in the phase using the equation: $[U]_f = K_s\Pi[c]_f^n$
  where $U]_f$ is the free concentration of U, K_s is the solubility constant, $[c]_f$ is the free concentration of each major ion in the solubility reaction and n is the stoichiometric coefficient in the reaction. This step has been performed correctly by SKB.

- To determine the solubility limit, the free U concentration then needs to be adjusted for the concentrations of the various aqueous species that contain U. The total U concentration in the aqueous solution can be determined using the following equation:
  $[U]_t = [U]_f + \Sigma_i K_i[U]_f\Pi[c]_f^n + 2\Sigma_j K_j[U]_f^2\Pi[c]_f^n + 3\Sigma_k K_k[U]_f^3\Pi[c]_f^n + \ldots$
  where K_i, K_j and K_k are the respective complex stability constants for monomers, dimers and trimers. In the calculations performed by SKB, the factor of 2 before the dimer expression and 3 before the trimer expression have been excluded. It is fortunate that U dimer or trimer species are not important in the determination of the solubility limit since the dominant species are $U(OH)_4(aq)$, $U(OH)_3^+$ and UO_2^+. Nevertheless, there may be conditions where these species do become important and the terms should be included.
- As indicated above, a number of U species have been excluded from the database. The dimer, $(UO_2)_2(OH)_2^{2+}$, for example, in the reference groundwater is a much more important species than the dimer that has been considered in the database, namely $(UO_2)_2CO_3(OH)_3^-$. It is recommended that the database be considerably modified to include those U species for which literature data are available but that have been excluded from the database. There are a number of carbonate species that have not been considered for U(IV) and U(V). Potentially, such species may become important when the pH is relatively high, such as in the ice melting groundwater scenario. Again, similar to Np and Pu, no species in which U is complexed by phosphate have been considered.
- As was the case for Np(IV) and Pu(IV), the potential for the formation of U(IV) colloids has not been discussed.

As a consequence of the deficiencies noted above, the potential exists that the uncertainties calculated for the solubility limits are understated, possibly by a significant amount under some scenarios. The review documented in Stenhouse et al. (2008) has already demonstrated that the uncertainties derived by SKB are understated and the above provides further evidence that this is the case.

5. Note on Some Relevant Properties of Swedish Groundwaters

By way of background information, the important influence of microbiological systems on natural aqueous systems is discussed in Appendix A. One of the key findings from the discussion in this Appendix is that the thermodynamic boundaries of biological systems and groundwaters, when plotted on an E_H-pH diagram, are similar. This observation was made many decades ago (Baas-Becking et al., 1960).

5.1 Swedish Groundwater Data: E_H-pH

Figure 2 shows a plot of data obtained from the analyses by SKB of Swedish groundwaters at the sites Forsmark, Laxemar, Simevarp, and Aspö, and contained in a spreadsheet of abstracted data (Bath, 2008). The abstracted data are provided in Annex A, and, as can be seen, are incomplete. In selecting data from the database, preference was given to field data.

The Swedish ground waters are reducing (E_H below 200 mV) and show rather high pH. A single observation falls below the limits set by the stability of water with respect to H_2 generation at 1 bar. This data point is for sample KLX02/1560 at Laxemar. As in a larger number of cases, the E_H value of this sample is given in brackets in the provided database table.

A simple statistical analysis of all 35 reported E_H values illustrates that they together can be interpreted as one set being normally distributed with mean x = -207 mV and sigma s = 80 mV. The only value showing some clear deviation is the above mentioned Laxemar value at E_H = -400 mV. This is shown in Figure 3.

Fisher (1925), the founding father of scientific data analysis (Aldrich, 1997), provided a thorough basis for the analysis of experimental data. The task of analysing groundwater data is not much different from the task Fisher faced at Rothamsted Experimental Station in analysing agricultural data. Fisher, however, was able to suggest designed experiments to unravel the effects of various methods and treatments on plant growth (Fisher, 1935). The hydrochemist / geologist is faced with a set of data that are unsuitable for randomisation. Nevertheless, modern data analysis tools allow an assessment of such data without reference to statistical models and assumptions on statistical processes beyond maximum likelihood.

An example is given in Figure 4 where the E_H-pH data provided by Bath (2008) have been analysed by the robust minimum covariance determinant estimator (MCDE) (Rousseeuw and van Drissen, 1999). The MCDE attempts to interpret a given multivariate data set by a maximum likelihood approach. The robustness is inferred from the breakdown level of 50 % for MCDE - the minimum value possible (implying maximum robustness). Thus, a model-free and robust classification tool like MCDE is a primary method of exploratory data analysis.

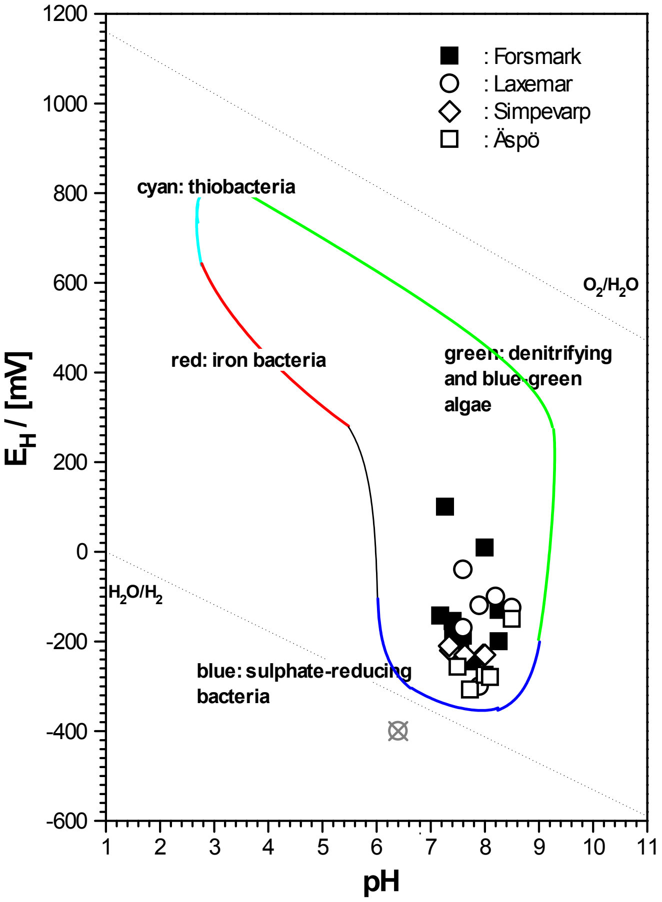

Figure 2: Oxidation-reduction potentials and associated pH pairs (n = 35) for Swedish ground waters at sites Forsmark, Laxemar, Simpevarp, and Aspö in comparison with the limits of natural environments (cf. Fig. A-2, Appendix A).

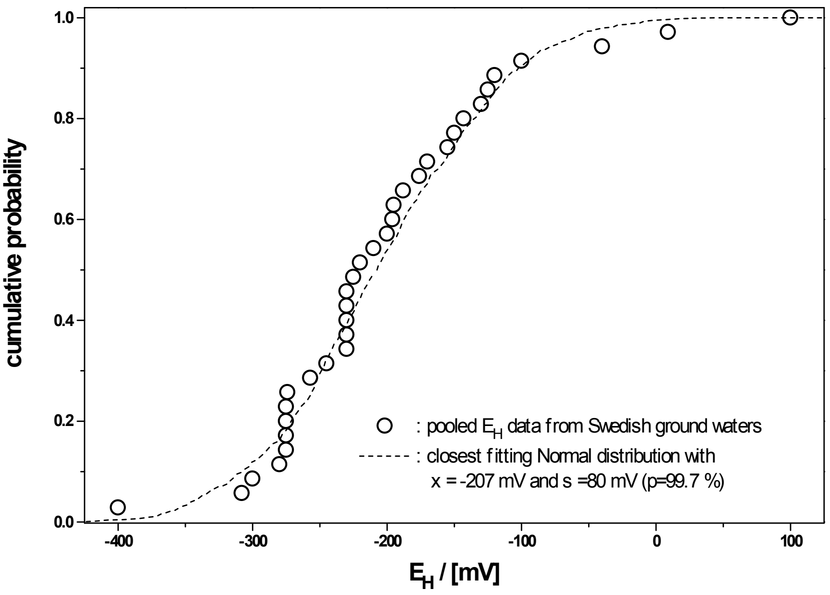

Figure 3: Cumulative distribution of pooled 35 E_H values of 35 ground waters from the four Swedish sites compared to the closest-fitting Normal distribution with mean *x* = 207 mV and standard deviation *s* = 80 mV. The probability that the data are normally distributed and that the deviations are random is 99.7 %.

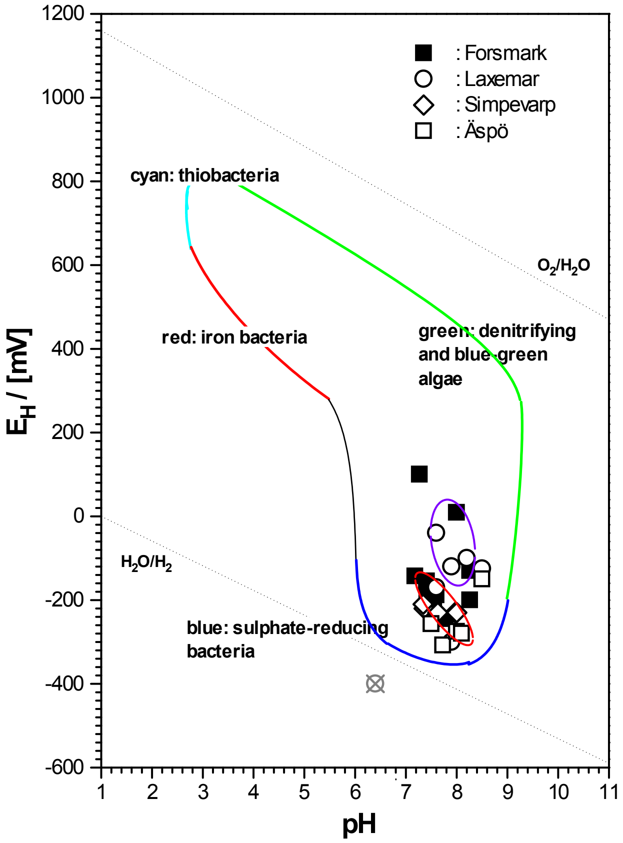

Figure 4: Interpretation of the reported E_H-pH data pairs from Swedish ground waters by robust minimum covariance determinant estimators (MCDE) (Rousseeuw and van Drissen, 1999) to assess associations between the data and to achieve an uncontaminated classification of the experimental data.

The breakdown level of a least-squares method refers to the number of outliers (outlying observations, extraneous data, contamination). The classical least sum of squared residual methods (e.g. liner regression) suffers from the large effects outlying observations have on the resulting statistics, e.g., slope and intercept of a regression line (Meinrath and Schneider, 2007). This strong influence is also termed a ‘masking effect’, because the extraneous observations tend to shift the least squares estimators in a direction to include the extraneous observation into the bulk of observations by:

a) shifting the mean; and
b) increasing the variance.

Robust methods, e.g., the least median of squares estimator (Rousseeuw, 1993), are not sensitive to extraneous data up to a certain percentage. Hence, the estimators obtained by least squares regression have a breakdown level of 0 %, because one single outlying observation in a data set will shift the estimators. The "least median of squared residuals" estimator however, tolerates up to 50 % of outlying observations. Up to this contamination level, the estimators are not shifted. Note that a higher breakdown level does not make sense. If ‘contaminations’ make up more than half of the data the question arises: “Which contaminates which?” High-breakdown methods are increasingly being used in practice, e.g., in chemistry, process control, and finance (Meer et al., 1991; Rouesseeuw, 1997).

The set of pooled experimental data is interpreted by MCDE allowing for 50 % outlying observations. In the bivariate data space (pH and E_H) a variance-covariance ellipse is obtained enclosing the data points compatible with a similar (least-squares) mechanism.

Other data, showing large Mahalanobis[1] distances under the minimum covariance assumption, are subsequently interpreted excluding the already interpreted data. Thus, the E_H-pH data of Swedish groundwaters are classified into two groups. The first group is given by the red ellipse, while the second group is centred about the blue ellipse. Two data points form their own (single member) groups: at (100 mV, pH 7.27) and at (-400 mV, pH 6.4). This classification is not based on any preliminary assumption except that the data are independent and represent random samples from a large population. This assumption corresponds to those underlying modern public polling strategies (Gallup, 1939).

Thus, the analysis indicates that the groundwater data are, despite the gaps in data, consistent. The presentation of the data, especially the large gaps and the pre-judgement of data (indicated, for instance, by bracketing some data), suggests that the data are not pure measurement data but have been edited according to some unknown criteria. It would be of importance to learn more about the editing criteria. On the basis of groundwater data analysis experience during the past 20 years, the observation can be reported that E_H measurements, for a variety of rather subjective but virtually never objectified reasons, are often considered as ‘unreliable’ or ‘potentially contaminated’. The practical experience, however, indicates that E_H values are usually no less reliable than, e.g., ICP-AES data on groundwater samples when the resolution power of the equipment (usually ±30 mV) is taken into account.

Even more than the 140 E_H-pH data pairs measured in the groundwaters sampled above the Gorleben salt dome between 1984 and 1989 (see Figure 5) could be nicely interpreted on the basis of the observations of Baas-Becking et al. (1960). In contrast to these waters with widely varying properties (in terms of organic material content, ionic strength, sulphate/sulphide etc.), the Swedish low ionic strength granitic formation waters seem much more homogeneous. The preceding analysis advocates trusting the measurements and interpreting the data only after a thorough data analysis. To illustrate this point, the following figure shows data collected during German uranium mining remediation activities of former East German-Soviet company WISMUT.

The few data points in Figure 5 at low pH falling outside the limits of natural aqueous systems are due to *in-situ* sulphuric acid leaching (Königstein sandstone mine). These conditions are definitively non-natural. All data were

---

[1] The Mahalanobis distance is based on correlations between variables from which different patterns can be identified and analyzed. It is a useful way of determining similarity of an unknown sample set to a known one.

collected during work on diploma theses or doctoral work by researchers generally unaware of the work of Baas-Becking et al. (1960).

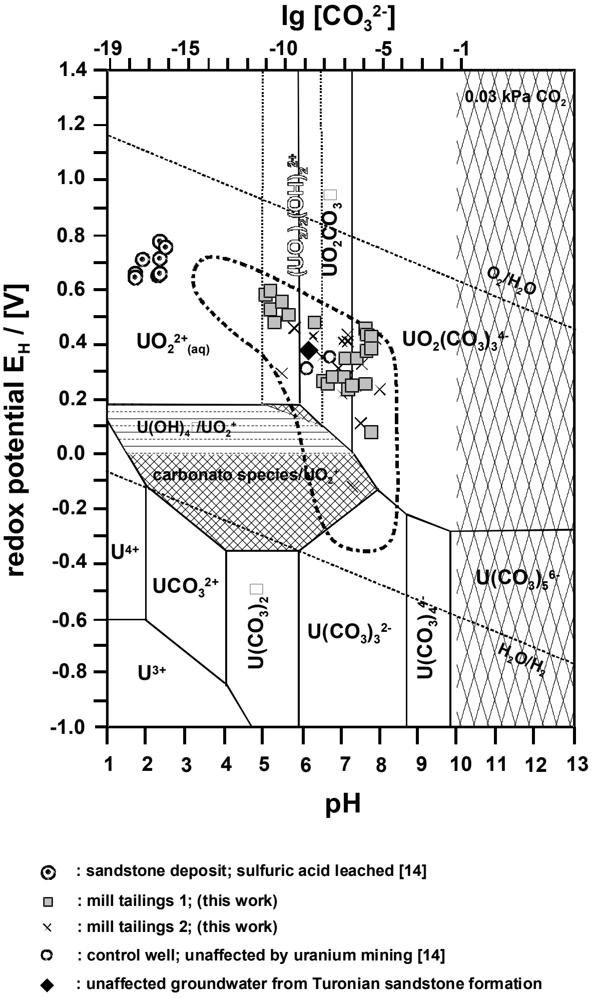

Figure 5: Field data from three different sites contaminated by former mining activities and (unaffected) control wells in Saxonia, Germany. The data are compared to the limits of natural aqueous environments (Baas-Becking et al., 1960) and the redox boundaries of uranium. Further details are given in Meinrath et al. (1999).

5.2 Carbonate in Groundwaters

CO_2 in the air dissolves in water forming successively HCO_3^- and CO_3^{2-}. These processes can be described in terms of chemical equilibria:

$$\lg[HCO_3^-] = \lg(K_H\ K_1) + \lg pCO_2 + pH$$

and

$$\lg[CO_3^{2-}] = \lg(K_H K_1 K_2) + \lg pCO_2 + 2\,pH\,.$$

The constants K_H, K_1 and K_2 are the Henry constant for dissolution of gaseous CO_2 in an aqueous medium, the first dissociation constant of H_2CO_3, and the second dissociation constant of H_2CO_3, respectively. These constants vary with ionic strength and temperature of an aqueous medium. However, under ambient conditions the variations in pH and pCO_2, the partial pressure of CO_2, are larger than those observed in K_H, K_1 and K_2. Thus by correlating pH with lg $[HCO_3^-]$, some conclusions can be obtained on pCO_2 for a given water. The ambient CO_2 partial pressure is about 0.0316 %.

pCO_2 in groundwaters is greater than that in the atmosphere as a result of production of CO2 by plant roots. Due to this source, pCO2 in soil from the first 20 cm below surface may reach up to 20 %. Meteoritic water percolating these soil layers saturates with CO2 during ground water recharge. Microbially-mediated degradation of organic matter may also contribute additional CO_2. Consequently, pCO_2 in groundwaters may reach 10 % in groundwater.

Figure 6 shows the results from the analysis of a number of groundwaters, with data pairs for pH and lg $[HCO_3]$ interpreted in terms of pCO_2. The data were collected routinely by four different groups who were unaware of this type of correlation at the time of data collection. Nevertheless, no data points fall below the lower line representing atmospheric CO_2 partial pressure, with pCO_2 rising close to 10 % for the reasons outlined above.

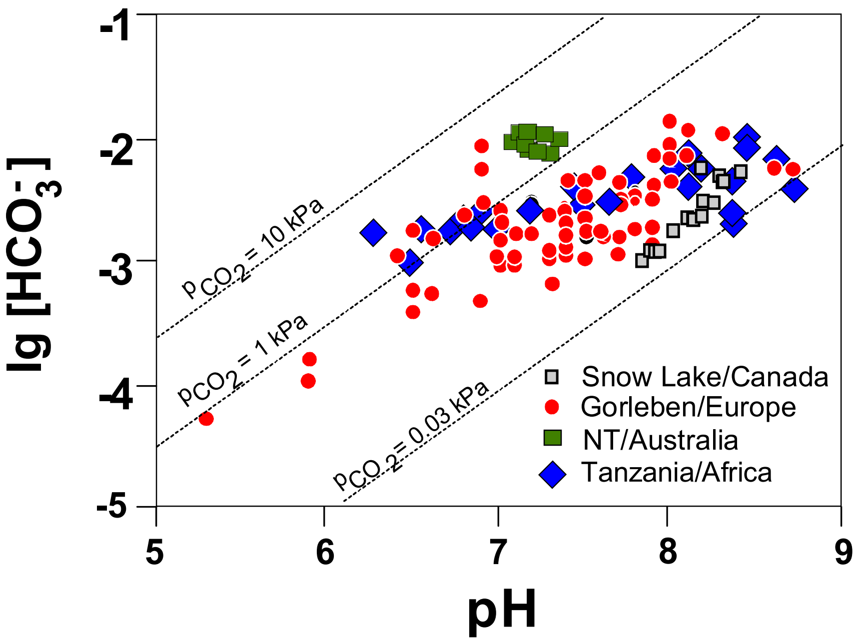

Figure 6: Correlation of measured HCO_3^- concentrations with measured pH and pCO_2. Experimental data from four continents are given representing a wide variety of conditions including about 140 data pairs from the formation above the Gorleben site.

5.3 Swedish Groundwaters: pH vs. lg [HCO_3^-]

Figure 7 shows a similar plot to that of Figure 6, but with data included for groundwaters collected from four sites in Sweden. Given the data presented in Figure 6, the observations made for the Swedish groundwaters are different in the respect that most of the data for all four sites fall below the limit of atmospheric CO_2 partial pressure. This may be the result of calcium release and proton consumption from aluminosilicate alteration in the deep bedrock (isolated from equilibration with atmospheric CO_2). Consequently, the resulting calcite precipitation will remove inorganic carbon from solution. Moreover, deep saline groundwater tend to have high concentrations of Ca^{2+} and more calcite is allowed to precipitate, which results in pH increases and [HCO_3^-] reductions.

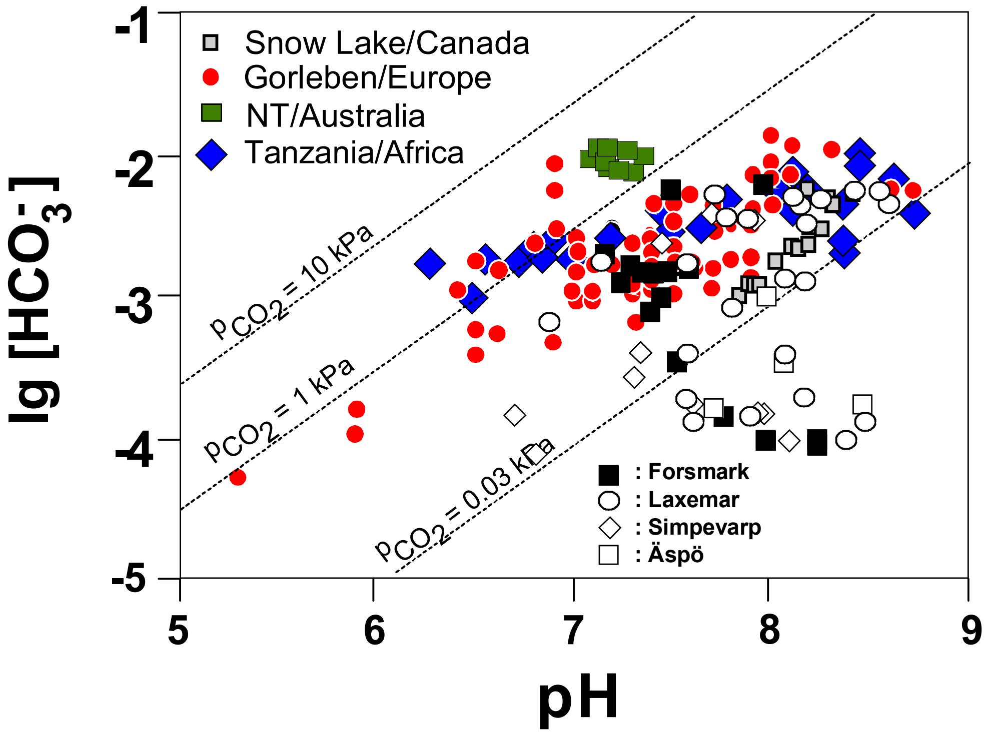

Figure 7: Correlation of measured HCO_3^- concentrations with measured pH and pCO_2. Experimental data from four continents are compared to the data pairs from the Swedish sites.

6. Data Reliability and GUM-Compliant Uncertainty Assessment of Sorption Data

In the context of good laboratory practice, the basis for the development of the international consensus document "*Guide to the Expression of Uncertainty in Measurement*" (GUM) is discussed in Appendix B together with the basic steps in the underlying procedure. Here, the GUM approach is applied to an uncertainty assessment of sorption data.

6.1 Sorption

6.1.1 Process

Within performance assessment of nuclear waste repositories, sorption plays an important role as a fundamental retardation process. Retardation may be quantitatively expressed by the (dimensionless) retardation coefficient R_f:

$$R_f = 1 + \frac{K_d \, \rho}{\phi_{formation}} \qquad (eq.\ 1)$$

where

ρ = density of stationary phase (kg/m^3),
$\phi_{formation}$ = porosity [-],
K_d = sorption or distribution coefficient (m^3/kg).

Despite extensive work being carried out to demonstrate the basis for more complex surface sorption models to be reliable predictors of retardation, the simple K_d model still dominates in nuclear waste repository performance assessment.

$$K_d = \frac{C_{sorb}}{[C_{sol}]} \frac{V_t}{m} \qquad (eq.2)$$

where

C_{sorb} = amount of A sorbed on the solid matrix [moles];
$[C_{sol}]$ = amount of of A in solution [moles];
V_t = volume of solution [dm^3];
m = mass of solid matrix [kg].

6.1.2 Uncertainty Analysis of Experimental Sorption Data

Equation (2) was used in the analysis of experimentally obtained data for the evaluation of a K_d value for the sorption of a radionuclide on granite (Andersson et al., 2008). The associated data in the report are accompanied by explanatory text indicating that the uncertainty analysis was not undertaken according to international consensus but following an individual procedure. The text from Andersson et al. (2008) describing the determination of the error associated with R_d, the experimental measurement of K_d, is provided in Annex B. For convenience, the final equation derived for the error on R_d is provided below.

$$\sigma_{Rd,g} = \frac{1}{m} \cdot \sqrt{\sigma_C{}^2 \cdot \left(\frac{V_{stam} \cdot V_{utt,n}}{A_{utt,n}} \right)^2 + \sigma_{A_{utt,n}}{}^2 \cdot \left(\frac{V_{utt,n}}{A_{utt,n}{}^2} \cdot \left(\sum_{i=1}^{n-1} A_{utt,i} - C \cdot V_{stam} \right) \right)^2 + \sigma_{L_d}{}^2 + \left(\frac{V_{utt,n}}{A_{utt,n}} \right)^2 \cdot \sum_{i=1}^{n-1} \sigma_{A_{utt,i}}{}^2}$$

(eq.4-25) from Andersson et al. (2008; see also Annex B).

Using this experimental work as an example, this section describes how the data and information provided in Anderssson et al. (2008) have been adapted to the international consensus GUM-compliant approach together with a brief discussion of the results.

In terms of constraints associated with this exercise, numerical values were not given in the text but provided on a separate worksheet. From this worksheet, the radioactive tracer was identified as ^{152}Eu. The concentration of the carrier was 6.4E07 M.

Based on eq. 4-25 in Andersson et al. (2008), an 'effective cause-and-effect diagram' can be derived, as shown in Figure 8, and the influence factors are included in Table 1. Note that Table 1 also contains those influence factors mentioned in the text but not further discussed.

Table 1: Influence factors considered in the evaluation of an R_d value for ^{152}Eu to Kivetty granite (0.045 mm – 2 mm fraction) in Olkiluoto saline water at pH 8.5.

Influence factor	***Symbol***	***u***	***v***
*Activity concentration of tracer*1)	C		*1*
Accumulated withdrawals of activity by n repeated samplings	$A_{utt,n}$		*1*
Product of wall sorption coefficient $R_{d,ref}$ *and "wall mass* m_w*"*	L_d		*1*
Sum of withdrawn activity	$\sum_{i=1}^{n-1} A_{utt,i}$		*1*
A_{tot}	A_{tot}		*1*
$A_{tot,\ ref}$	$A_{tot,\ ref}$		*?*
Hydroxide concentration	*[OH]*		*?*
Ligand concentration	*[L]*		*?*
Background	---	---	---

[1] *Note: C is used for two quantities: the tracer concentration in the reference (unfortunately a mean concentration is used; cf. eq. 4-11 in Annex B), and the concentration in the tracer stock solution (cf. eq. 4-12 in Annex B).*

In addition to the influence factors summarized above the "*experimental limitation where the amount of adsorbed material is measured indirectly, by measuring what is left in solution und using the mass balance*" is mentioned without further recurrence to this crucial step in the uncertainty assessment of a K_d value.

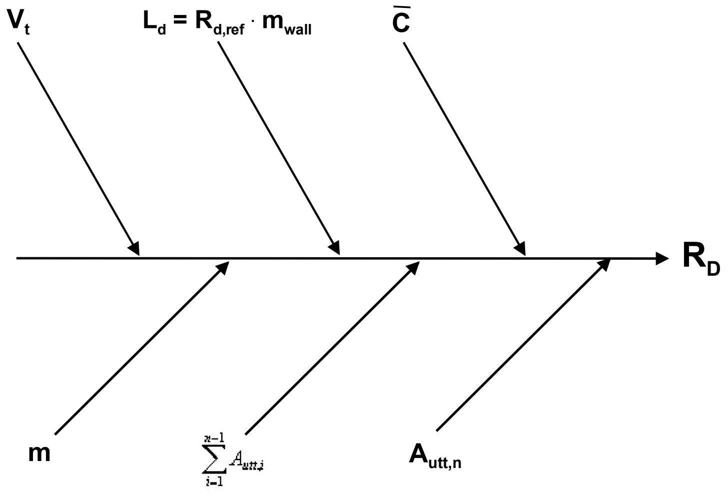

Figure 8: Approximate cause-and-effect diagram for the evaluation of R_d values for the sorption of ^{152}Eu to Kivetty granite (0.045 mm – 2 mm fraction) in Olkiluoto saline water at pH 8.5.

The extracted text in Andersson et al. (2008; see Annex B) is rather difficult to follow from a quality assurance (QA) perspective. The motivation behind the individual steps is mostly hidden and the summary error (in R_d) in eq. 4-25 (Annex B) is almost untrackable.

The researchers were faced with the same three tasks mentioned in the introduction to Appendix B:

- The need for extensive documentation of the individual steps.
- Keeping track of various systematic and random uncertainty contributions (in fact, the discussion either does not address the respective contributions, or ascertains that the magnitude of the variability is negligible, or urges caution instead of presenting a repeatability or reproducibility.
- Finding a suitable compromise between the quest for conservatisms and the need to have small overall uncertainties.

The abstracted text in Annex B, therefore, highlights the need for an internationally-accepted convention to communicate on measurement uncertainty as is provided by the GUM and supplemented by the various guides from EURACHEM (2000, 2002).

To emphasise this point, reference is made to the first equation defining the R_d, the quantity of interest. In this case, A_{sorb}, the activity sorbed on the solid, must be evaluated from the difference between two other quantities, quantities, A_{aq} (the activity of radionuclide in the aqueous phase) and A_{tot} (total amount of radionuclide added initially), both of which are affected by uncertainty. Hence, a term like

$$\mathrm{A_{sorb} = (A_{tot} - A_{aq})} \qquad \textit{(eq. 3)}$$

may be expected. Subsequently

$$R_d = \frac{(A_{tot} - A_{aq})\quad V}{A_{aq}\quad m} \qquad \textit{(eq. 4)}$$

Note that the evaluation of σ_{Rd} in eq.4-25 (Annex B) is not applicable for error propagation involving product or quotient operations.

Furthermore, the (unspecified) concentration of the carrier plays an important role because Eu(III) is a rather insoluble compound at pH 8.5. Eu(III) hydrolyses and coordinates to carbonate. In assessing the solution conditions for this hydrolysable ion, the presence of 'saline water' as solution phase should be mentioned. Hence, there are additional issues in estimating a reasonable solution pH. Commercially available traceable pH calibration buffers are valid up to an ionic strength I = 0.3 mol only. The ratio of inactive Eu to ^{152}Eu sets a limitation on the total activity to be added to the sample. Hence, the information provided is not sufficient to judge the respective data. The initial activity of ^{152}Eu, A_{tot}, is not given. Consequently the complete analysis cannot be retraced. However, the rather sensitive relationship among the different activity contributions in Eqs. 3 and 4 can be addressed.

Three situations can be assumed:

a) low sorption tendency: $A_{aq} \sim A_{tot}$
b) high sorption tendency: $A_{tot} \sim (A_{tot} - A_{aq})$
c) intermediate sorption tendency: $A_{aq} \sim (A_{tot} - A_{aq})$

In case a) the measurement uncertainty is crucially dependent on the counting uncertainties in A_{aq} and A_{tot} because the quantity of interest, A_{sorb}, is obtained as the small difference between two large numbers. In some situations even negative differences may result. This situation should have been observed in the case of the wall sorption study component of the experimental work under review here.

In case b) the count rate in the aqueous phase is very small and, hence, close to background activity. Background counting variations cannot be neglected - and even determine the final result.

Situation c) is the most appropriate where the activity divides equally between the sorbed and the aqueous state. This situation can be adjusted within rather narrow limits by fixing the ratio $V{:}m$. However, because these amounts usually cannot be varied over orders of magnitude, the experimental conditions are mostly determined by the system under study. A lump treatment of measurement uncertainties for K_d values ("*...are in the order of...*") is therefore inappropriate.

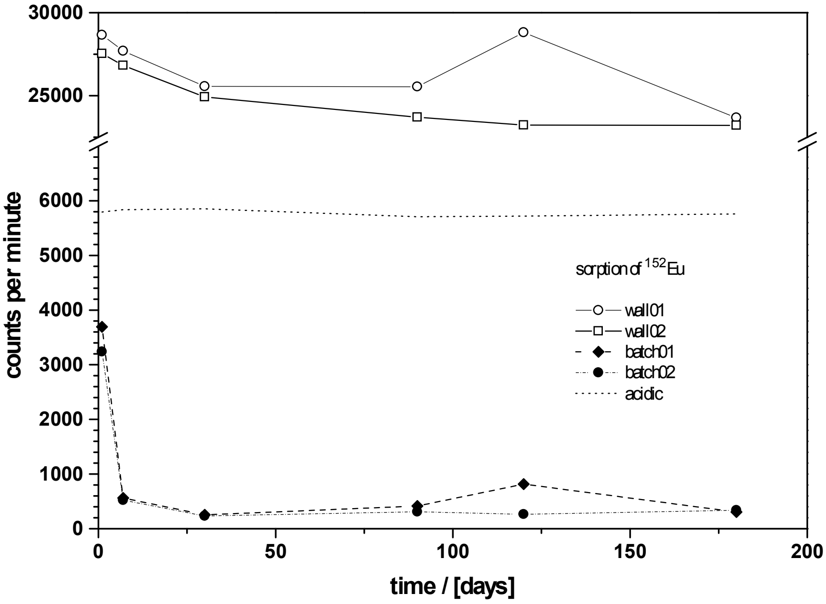

Figure 9: Experimental data on ^{152}Eu sorption on Kivetty granite (0.045 mm – 2 mm fraction) in Olkiluoto saline water at pH 8.5.

Note: The wall experiments study sorption to container walls in the absence of granite, while the 'acidic' experiments are aimed at determining A_{tot}, the amount of ^{152}Eu present originally. The batch experiments give A_{aq}. The count rates for the batch experiments are rather low and, in contrast to the count rates of the other quantities, not corrected for background. Nevertheless, a count rate of a few hundred counts per minute is rather close to the background count rate (stated in Andersson et al. [2008] as 75 cpm, without variability). Given the above relative activities, the situation becomes close to situation b).

The foregoing discussion illustrates the specific difficulties of an experimentalist in quantifying and communicating data uncertainties and a reader in re-assessing the statements in a report without guidance by a common convention.

6.2 Assessing a Sorption Coefficient K_d According to the GUM Convention

Here, an example is given of a GUM-compliant measurement uncertainty assessment of a K_d value. In this example, ^{241}Am is used as a relevant radioactive nuclide, and in this case, the issue of carrier/tracer ratio does not arise.

6.2.1 Step 1: Specify quantity being evaluated

The quantity K_d is evaluated according to;

$$K_d = \frac{Am(III)_{sorb}}{Am(III)_{sol}} \frac{V_t}{m} \qquad (eq.\ 5)$$

A_{sorb} : = amount of substance A sorbed to solid matrix [moles];
A_{sol} = amount of substance A in solution after equilibration [moles];
V_t : = total solution volume [dm^3];
m : = mass of solid matrix [kg].

The sorbed amount of ^{241}Am, $Am(III)_{sorb}$, has to be evaluated from the difference between the total amount $Am(III)_0$ added, and the amount $Am(III)_{sol}$ obtained in solution after equilibration. This yields

$$K_d = (\frac{Am(III)_0}{Am(III)_{sol}} - 1)\frac{V_t}{m} \qquad (eq.\ 6)$$

6.2.2 Step 2: Identify possible influences

The possible influence quantities have to be identified. Possible factors that may influence the numerical result for K_d are:

a) Temperature.
b) Composition of the solution and its change during equilibration period.
c) Activities of ionic solution components and the respective variations during equilibration period.
d) Microbial influences (sterile conditions in aqueous electrolyte solutions at common laboratory conditions are virtually impossible).
e) Identification of sorbed species.
f) Solubility limits.
g) Sorption to container walls.
h) Volume operations.
i) Sampling procedure (e.g., ultrafiltration).
j) Total volume V_t at sampling times.
k) Porosity of matrix material and its variations during equilibration time.
l) Homogeneity of matrix (e.g. clays in and on the pores of granitic materials).
m) Accuracy and precision of a balance.
n) Background of radiation detector.
o) Counting statistics of radiation detector.
p) Calibration of counting device.

Thus, the appropriate cause-and-effect diagram is shown in Figure 10.

6.2.3 Step 3: Identifying relevant influences

The discussion below addresses those influence quantities that have been identified as relevant:

(a) $\boldsymbol{V_t}$

The total volume of the aqueous phase will change in the course of the experiment for several reasons. Firstly, liquid will be sampled during the equilibration time in order to assess the progress of the reaction in the container. Furthermore the matrix may uptake solution into its pores. Water will evaporate or be carried with a gaseous stream applied to maintain a defined atmosphere.

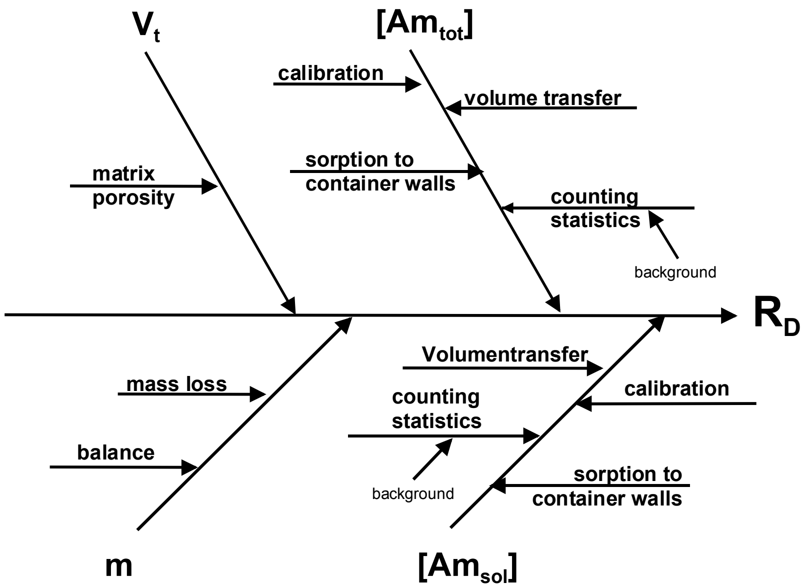

Figure 10: Cause-and-effect diagram for the sorption of Am(III) to a granitic ground water.

(b) ***m***

The mass of the solid phase cannot be determined with an arbitrary accuracy. It is possible to use a calibrated balance with high accuracy. But geological materials have the property of containing water (crystal water, pore water, adsorbed water). Thus, there is a general problem of defining exactly what is encompassed by the term ‘solid matrix’. In the case of a granitic sample being appropriately dried in a desiccator, the water content may be considered to be low.

The exact amount of solid matrix is not only determined by the weighed amount subsequently taken from the balance. Some material will not reach the equilibration vessel. In the case of fine-grained material, the amount on the balance and the amount reaching the vessel may differ due to material remaining on the spatula and/or glass equipment used to transfer the material. In the case of macroscopic amounts (order of a gram), such effects will be below 1 %. For K_d determinations, *V:m* ratios of 0.1-10 are typically applied (e.g., 10 mL aqueous phase and 1 g solid). In the case of Am, however, a K_d of 500 dm^3 kg^{-1} is expected and high K_d values require a high excess of aqueous volume because even small amounts of solid are able to remove considerable amounts from the solution by sorption. In this example, it will be assumed that 0.1 g of a dried solid granite sample is equilibrated with 0.1 dm^3 of groundwater. Therefore, the uncertainty in the amount of solid phase is reasonably 5 %.

(c) ***Am(III)₀***

The initial activity $Am(III)_0$ is assessed by liquid scintillation counting of its α activity. Am(III) forms various solid phases ($Am(OH)_{3,s}$, $AmOHCO_{3,s}$, and $Am_2(CO_3)_3.xH_2O$). Under laboratory conditions at atmospheric CO_2 partial pressure, $AmOHCO_{3,s}$ may be assumed as the solubility-limiting solid phase.

The total amount of Am(III) in the vessel has to be safely below the solubility limit of this phase, in which case the uncertainties in the solubility limits of Am(III) have to be taken into account. In order to keep this example focused, the data from an investigation of Ekberg et al. (2003) will be used, where the uncertainties in the solubility limits of Am(III) phases have been combined with sensitivity analyses to arrive at a reasonable estimate of these uncertainties. In Table 2, the respective uncertainties used for the assessment of Am(III) solubility limit assessment from Ekberg et al. (2003) are given.

Table 2: Influence quantities and associated uncertainties in the assessment of uncertainty in Am(III) solubility according to Ekberg et al. (2003).

Branch	**Cause / Effect**	**Uncertainty**	**u_c**
^{241}Am(III)$_O$			±0.7%
	$t_{1/2}(^{241}$Am)	0.14%	
	counting efficiency	0.68%	
	volume	0.2% - 1%	
lg [OH$^-$]			±0.06$_1$
	pH	±0.035	
	lg K_W	±0.05	
temperature			negligible
ionic strength			negligible

The resulting uncertainty distribution of the Am(III) solubility is shown in Figure 11.

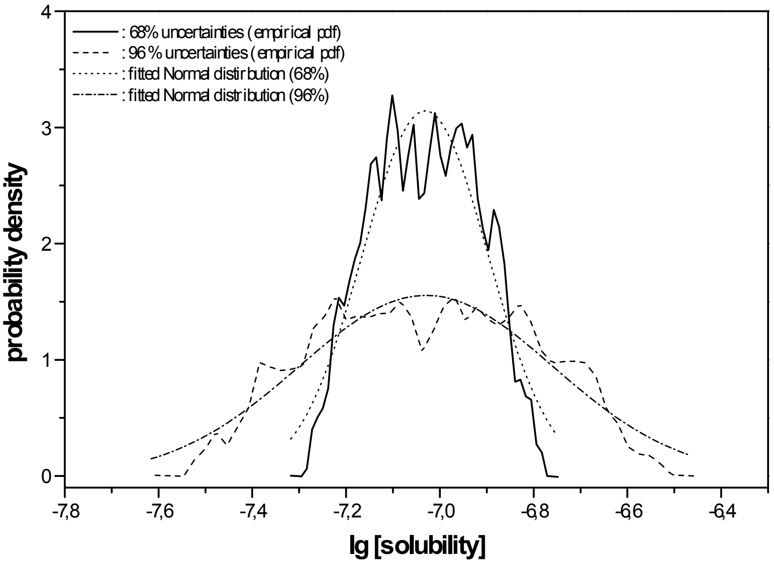

Figure 11: Distribution of the $AmOHCO_{3,s}$ solubility limit in a low ionic strength water (from Ekberg et al. 2003).

Fitting a Normal distribution to the solubility limits (using Kolmogorov-Smirnov criterion) and accepting a 5 % risk that the solubility limit is actually below this confidence limit, a solubility limit of $2.5 \bullet 10^{-8}$ mol Am(III) dm^{-3} must not be exceeded. Because it is reasonable to maintain a 'safety distance' to avoid local precipitation at surfaces, the amount of Am(III) applied should not exceed $2.5 \bullet 10^{-9}$ mol dm^{-3}. It should be mentioned that calculations of solubility limits, as shown in Figure 11, require very elaborate considerations and calculations. Thermodynamic data for complex formation with water constituents are essential. In addition such calculations are vital in assessing the amount of sorbing material being stabilised in aqueous solution by complex formation. Such aspects are only mentioned here but not further elaborated on for the sake of brevity.

Due to the half life of ^{241}Am of 426 a, a maximum activity of ~$7.5 \bullet 10^{4}$ Bq dm^{-3} is obtained. Sampling 100 µL therefore will result in only ~8 Bq. Thus a minimum of 500 µL should be sampled to achieve reasonable counting statistics. Sampling 0.5 mL each time from a 100 mL total sample will, of course, influence V_t.

The concentration determination of ^{241}Am itself depends on a number of influences. Sorption to container walls is an example. Due to trace level concentrations (that cannot be increased because of solubility constraints) several per cent of the material can disappear from the solution without being sorbed on the matrix. Furthermore, the volume operation, e.g., using an Eppendorf pipette at the sub-mL region, is associated with a rather large uncertainty of 1 % - 3 %.

Calibration of a scintillation detector usually is done by a calibration standard solution. Associated uncertainties are up to 3 %. Hence the observed count rate will fall between 97 % and 103 % of the expected rate.

Counting statistics becomes more significant the lower the absolute count rate. This effect is commonly compensated by increased counting time. The longer the counting time and the lower the count rate the higher becomes the influence of the background rate. Well-maintained scintillation counters have a background count rate of ~2 Bq–5 Bq. At counting levels of 80 Bq, however, this contributes already 3 % - 7 %! Other influences like electrostatic charging of the counting vial are not considered further here.

d) ***Am(III)$_{sol}$***
The amount of sorbed material is usually calculated from the difference between the total Am(III) added and the aqueous amount of Am(III) after establishment of a steady concentration. The influence quantities are the same as described under c). The relationship between count rate and background, however, is worse because the background counts remain constant but the remaining Am(III) in solution is considerably lower (if sorption occurs). Assuming a reduction of Am(III) by 50 % due to sorption, the uncertainties increase to 6 % - 15 %.

6.2.4 Step 4: Quantify uncertainty

Uncertainty in ratio V m^{-1} (= *K*):

$$u_K = \sqrt{(0.01)^2 + (0.05)^2} \approx 0.05 \qquad \textit{(eq. 7)}$$

results in the following value of *K:*

$$K = \frac{100\ ml}{0.1\ g} = (1000 \pm 20)\ ml\ g^{-1} \qquad \textit{(eq. 8)}$$

Figure 9 suggests that uncertainties in background count rate and counting statistics add. Hence application of error propagation yields:

$$u_{Z,0} = \sqrt{(0.03)^2 + (0.04)^2} = 0.05 \qquad \textit{(eq. 9)}$$

A count rate in the given activity range is associated with a relative uncertainty of about 5 %. This uncertainty together with other uncertainties given in Table 3 combine:

Table 3: Influence quantities and associated relative uncertainties.

Influence quantity		**Relative uncertainty in %**	**Comment**
V_t		1 %	Global; Uncertainty resulting from 10 samplings (~5 mL) and humidity absorption of the dried granite matrix
m		5 %	Rather elevated K_d of about 500 $dm^3\ kg^{-1}$ causes large $V:m$ ratios for matrix mass m below 1 g.
$[Am(III)_0]$	calibration	3 %	
	volume transfer	2 %	
	background	4 %	
	counting statistics	3 %	
	sorption to container walls	2 %	
$[Am(III)_{sol}]$	calibration	3 %	
	volume transfer	2 %	
	background	3 %	
	counting statistics	8 %	Small activity in the solution after equilibration causes poor counting statistics
	sorption to container walls	2 %	

$$u_{sol} = \sqrt{(0.05)^2 + (0.02)^2 + (0.02)^2 + (0.03)^2} = 0.065 \qquad \textit{(eq. 10)}$$

The same procedure follows for quantity $Am(III)_{sol}$. However, the influence of the background rate uncertainty is higher due to the lower absolute count rate:

$$u_{Z,sol} = \sqrt{(0.03)^2 + (0.08)^2} = 0.09 \qquad \textit{(eq. 11)}$$

It follows for the combined uncertainty u_{sol} for Am(III) remaining in solution:

$$u_{sol} = \sqrt{(0.09)^2 + (0.02)^2 + (0.02)^2 + (0.03)^2} = 0.1 \qquad \textit{(eq. 12)}$$

It should be mentioned that the influence in the uncertainty in the amount of Am(III) attached to container walls should be higher compared to $Am(III)_0$. In this illustrating example, this effect will be neglected.

Following the respective procedures for the ratio Am(III)$_0$ Am(III)$_{sol}^{-1}$ yields:

$$u_{conc} = \sqrt{(0.065)^2 + (0.1)^2} = 0.12 \quad \textit{(eq. 13)}$$

hence a relative uncertainty of 12 %.
The total uncertainty from this procedure for a K_d of Am(III) to a granitic matrix is obtained from a combination of u_{conc} und u_K

$$u_{K_D} = \sqrt{(0.12)^2 + (0.05)^2} = 0.13 \qquad \textit{(eq. 14)}$$

Thus a GUM compliant K_d is (500 ± 65) dm^3 kg^{-1}.

Accepting the expansion factor $k = 2$ (requiring a rather large number of repetitious determinations) leads to

$$K_d = (500 \pm 130)\ \mathrm{dm^3\ kg^{-1}}\ (k = 2) \qquad \textit{(eq. 15)}$$

This example is based on simplifications because the available experimental data are inadequate to evaluate a GUM-compliant uncertainty estimate. For example, effects of the sampling procedure (e.g. ultra-filtration) have not been taken into account. However, the advantages of the GUM convention can easily be recognised. Subsequent criticism of the data can be either rebuffed or used to improve the procedure. Comparability with data obtained for the same system under different conditions, different locations, at different times and by different people can easily be assessed.

To avoid over-interpretation of this example, it is emphasised that mainly statistical variation has been addressed. Variability in the experimental procedures and the sample materials cannot be assessed without the necessary experimental details. Round robin studies are a suitable tool for quantifying such variance.

7. Data Variability and the Use of the Triangular Distribution

7.1 Context

One of the more unusual findings in SKB reports is the occasional reference to triangular distributions (SKB, 2006a; pages 199, 406 [table], 409, 427 [table], and 430). The triangular distribution is, at least in a scientific and technical context, used much less frequently than the well-established Normal distribution, the latter based on almost 300 years of experience in reasoning on the nature of chance. By way of background information, Appendix C discusses the characteristics of the triangular distribution.

A search of the literature indicates that the relatively recent interest in the triangular distribution is mainly due to its inclusion in mathematical and statistical software packages like @RISK and Crystal Ball. Examples for specific application fields for the triangular distribution are:

- Availability of only very small data sets.
- Data distributed between known upper and lower limits, where the location of the most likely outcome is known (otherwise the uniform distribution would be adequate).
- Decision-making in the business field (e.g., exploration efforts in geology have been stressed on several occasions).
- Program Evaluation and Reporting Technique (PERT): PERT primarily uses the beta distribution[2] to model planning and production times within a project. The triangular distribution is considered to be an adequate simplification in this context.

7.2 Issues Concerning the Use of the Triangular Distribution

A number of key issues are relevant to some reservations regarding the use of the triangular distribution in favour of the Normal distribution:

(1) Tail Probabilities (with an emphasis on risk analysis)
The use of triangular distributions to model scientific data or data from scientific investigations, differs from the Normal distribution mainly due to the emphasis put on the distribution tails. While the Normal distributions allows, with very low but non-zero probability, the occurrence of observations very far from the distribution centre, the triangular distribution does not allow for observations above d_o and below d_u, i.e., outliers are not considered. Outlier

---

[2] Beta distribution = family of continuous probability distributions.

analysis, detection and handling are important issues when applying distributions.

As stated above, within a statistical model based on triangular distributions, outliers are not foreseen. Reality, however, shows a different behaviour (Beckman and Cook, 1983) - the occurrence of outliers (or extraneous observations) is commonly more frequent than even the Normal distribution allows. Within risk analysis, the tails of a distribution and outlying observations play a critical role. Risk analysis focuses on the assessment of rather unlikely incidents represented mainly by the tails of the distributions. In particular, the performance assessment of a high-level nuclear waste repository focuses on a numerical limit for unusual states of a repository possibly causing a failure due to occurrence of conditions for which the repository is not designed. *Such unusual states are represented by the tails of a probability distribution*. For this reason, it is important to ensure that the tails are not ignored.

(2) Uncertainty Propagation

The characterisation of data in terms of a distribution may provide some illustrative insight into the data. Normally distributed data, for instance, may be expected from processes that are independent of each other, each having independent but constant variances. However, distributions become of major interest when they are combined, e.g. in the case of error propagation. For the Normal distribution, rather simple relationships exist for combining the standard deviations of two distributions. Since the combination of Normally distributed data again results in a Normal distribution, propagation of uncertainties can be made in terms of the variability parameter s of the Normal distributions. Given two Normally distributed parameters with means A and B, and the respective standard deviations s_A and s_B, the following simple rules hold:

$$\mathrm{s(A + B) = s(A - B)} = \sqrt{\mathrm{s_A}^2 + \mathrm{s_B}^2}$$

and

$$s(A \cdot B) = A \cdot B \sqrt{\left(\frac{s_A}{A}\right)^2 + \left(\frac{s_B}{B}\right)^2}$$

$$s(\frac{A}{B}) = \frac{A}{B} \sqrt{\left(\frac{s_A}{A}\right)^2 + \left(\frac{s_B}{B}\right)^2}$$

Similar rules exist for powers and functions. A search of the literature did not reveal analogous relationships for the uncertainty propagation of triangular distributions. Hence, uncertainty propagation for triangularly distributed data needs to be done, for instance, by Monte Carlo sampling.

(3) Monte Carlo Sampling and Coverage

With Monte Carlo (MC) methods, the problem of coverage comes into play. For any distribution with a central tendency, such as the triangular distribution and the Normal distribution, the majority of MC samples will be close to the expectation value. Values closer to the extreme values or the tails will have a lower probability of being included in a sample of finite size. Hence, in order to model a triangular distribution with central tendency by MC samples, the probability of including an extreme value, both d_u and d_o, into a MC sample is virtually zero because the probability density at these points is zero. Hence, the extreme values of an MC sample will always be narrower than the extremes of the original triangular distribution. Thus, repeated application of sampling from a triangular distribution will in fact underestimate the position of d_o and d_u for the combined distribution, if appropriate measures are not taken.

The confidence regions of a Normal distribution are well known. Using a standard Normal distribution, the area under the curve between $-s$ and $+s$ is about 0.68. The area between the $2s$ limits is approximately 0.97, while the area under the curve with the $3s$ confidence limits is 0.997. Using small sample distributions, appropriate values from the Student t distribution have to be applied taking into account that the mean is actually Student t distributed. 'Appropriate' means that the respective degrees of freedom have to be considered. The appropriate values for $t_{df,\alpha}$ where df is the degree of freedom and α is the desired confidence level, can be conveniently calculated or read from a table.

In order to ensure that at least one sampled value falls beyond the α tails of n Normal distributions with a probability of p, the minimum number N of total samples to be collected in a pure MC approach is obtained from the relationship:

$$p < (1 - \alpha^n)^N.$$

This relationship indicates that for $p = 0.99$, $\alpha = 0.95$ and $n = 3$, N is 35840. Thus MC sampling for propagating Normal distributions is not feasible even for a modest number of distributions to sample from. For the triangular distributions, such relations would be of considerable interest with reference to the relevance of tail probabilities in risk analysis.

(4) Confidence Regions

The confidence regions for Normally distributed parameters can be plotted conveniently. The confidence regions have an elliptical shape given by

$$(A - A')^T \, \frac{(\mathbf{X}^T \mathbf{X})}{s^2} (A - A') = P \, F_{P,n-P,\alpha}$$

where $\boldsymbol{A'}$ is the vector of mean values, the superscript T denotes a transposed vector (or matrix) while $\boldsymbol{X}^T \boldsymbol{X}$ is the design matrix. Var(A') = $s^2 \, (\boldsymbol{X}^T \boldsymbol{X})^{-1}$ is the variance-covariance matrix. The residual mean square error s^2 is obtained as the sum of squared residuals between estimates $\boldsymbol{A'}$ and the experimental data divided by the degrees of freedom. P gives the number of parameters while $F_{P, n-P, \alpha}$ is obtained from Fisher's F distribution with P and n-P degrees of freedom at a confidence level α. Figure 12 provides an example where the joint confidence region about a mean value is shown for two Normally distributed parameters $ß_1$ and $ß_2$ is given.

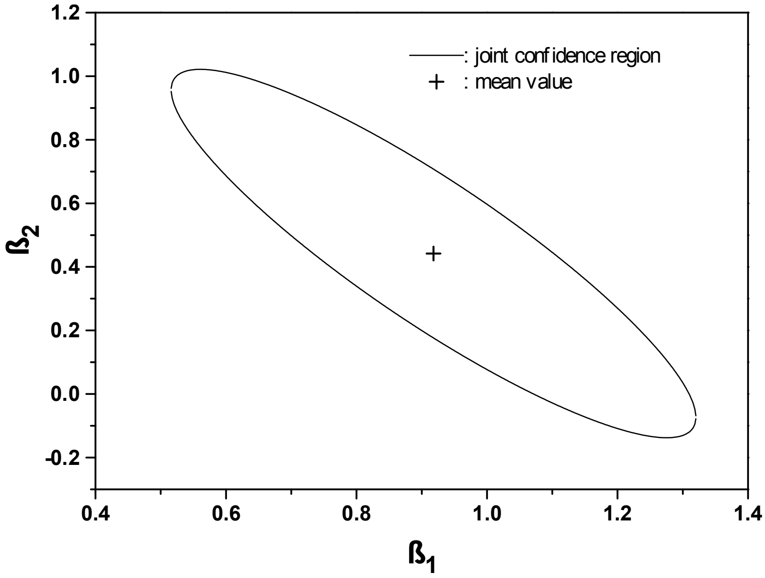

Figure 12: Joint confidence region at some confidence level α of two parameters $ß_1$ and $ß_2$ about the mean.

The above topics (1) – (4) underscore that the Normal distribution has, due to the central focus given to it by the CLT combined with almost 300 years of intense research about its properties, a series of features which are not available for other distributions.

7.3 Conclusions – Remaining Questions

Thus, if a distribution other than the Normal distribution is to be preferred to describe variance and variability, a solid understanding of the properties of the chosen alternative distribution is necessary. With regard to the use of triangular distributions in SKB's documentation for SR Can, and given the discussion above, several questions are pertinent:

1. For what types of problem is the triangular distribution applied and what are the reasons for replacing the Normal distribution?
2. According to which numerical procedure(s) are the parameters of the triangular distributions estimated?
3. Have alternative distributions (e.g. the Weibull distribution, as discussed in Appendix C-3) been considered?
4. How is the issue of outliers handled when interpreting datasets in terms of triangular distributions? Are the extremes (d_u and/or d_o) just set to the extreme observations?
5. How are joint confidence regions presented? Are graphical representations of triangular distributions displayed at all?
6. Are the quantiles of the various triangular distributions known?

7. How is the number of realisations to be sampled from triangular distributions estimated in order to achieve a certain coverage level? How is a proper representation of the complete sampling space in the resulting output distribution(s) ensured?
8. What are the advantages and disadvantages of using triangular distributions from SKB's perspective? Do comparative assessments (case studies) with alternative distributions exist?

8. Transport Properties in the Geosphere: Additional Input from SKB

8.1 SKB Responses to Issues Raised

Many of the issues raised in our previous report (Stenhouse et al., 2008) were addressed at the meeting / workshop held in May. Furthermore, SKB subsequently provided an additional document (Selroos, 2008) with input and specific responses to issues raised in the 2008 report. The relevant information is provided in Table 4 and includes the original comment, SKB's response and the response of the SSM reviewer.

Generally, the responses indicate that SKB is continuing to provide experimental data to lend support to many of the conclusions presented in Liu et al. (2006). Based on these responses, additional technical documents either published or about to be published, will help clarify some of SKB's data selection in the area of matrix diffusion.

Table 4: SKB's responses to comments on radionuclide transport in the geosphere.

Summary of original comment (page / Stenhouse et al. 2008)	SKB response	SSM External Reviewer Comment
Equation 1: $De = D_W(\varepsilon\delta/\tau^2)$ (Page 11) Equation 5: $De = D_W F_f$ (Page 41 – also below) The formation factor, *F*, is an overall geometric factor that takes into account porosity as well as constrictivity (cross-sectional area of pores) and tortuosity (true length of pathway) of the pores.	If the formation factor is defined as purely a geometric factor (as it usually is), equations 1 and 5 only apply simultaneously if there is no interaction between the solutes and pore walls (other than geometric hindrance). As the solutes and pore walls are electrically charged this is not the case in crystalline rock, in which case corrections are needed. At present there is no consensus how to do this within the scientific community. Still this problem needs to be, and is being, addressed in SR-Site.	Comment understood and accepted. It will be interesting to read SKB's approach on this topic in SR-Site.
It would be useful to see a comparison of formation factors determined using electrical and more traditional techniques. (Page 42)	Such results are given in *Löfgren M., Neretnieks I., 2006. Through- electromigration: A new method of investigating pore connectivity and obtaining formation factors. Journal of Contaminant Hydrology, Vol. 87, pp. 237–252.* Results show only minor deviations between the measurements. Similar measurements are being planned by SKB to obtain further information on possible deviations.	The results and discussion in the paper cited support SKB's arguments. Additional data in this area from various sources will help consolidate the measurement of formation factor by electrical methods.

It is possible that electrical methods based on the application of an *alternating* current do not necessarily reflect the movement of ions, but may also be due to the conduction of electricity across, for example, metal oxide minerals. (Page 42)	This question is also addressed in *Löfgren M., Neretnieks I., 2006 [as above]*. Electrically conducting minerals blocking the pores but allowing propagation of current was found insignificant. Also, phase-angle measurements show little anomalous conduction due to electrically conducting minerals (e.g. Thunehed, 2007, SKB P-07-51)	Comment accepted. The topic is also addressed in the more recent SKB report R-08-48. Data from a variety of sources and a range of mineralogies would help consolidate SKB's findings.
Evidence supporting the assumption of porewater equilibrium with freely flowing groundwater (fractures) (Page 42)	By comparing electrical conductivity of free groundwater extracted from fractures with that of pore water leached from drill core samples (e.g. Waber and Smellie, 2007, SKB SKB P- 07-119) it has been shown that the assumption of equilibrated pore water and free groundwater is valid to sufficient degree. Below this table a figure from Löfgren, 2007, SKB P-07-138 is given showing data from free groundwater (triangles) and pore water (rings) for borehole KFM01D and KFM08C. Comparing to other uncertainty this is important but not overwhelming.	The data provided are informative and help support SKB's assumption "*to a sufficient degree*". Additional data in this area from other sources will increase confidence, although it is accepted that the uncertainty associated with this assumption is small compared with other uncertainties.
"*In situ groundwater electrical conductivity measurements*" – were such measurements not carried out in the laboratory rather than in situ? (Page 43)	The electrical conductivity is measured in-situ (in the borehole) with the Posiva difference flow meter. In the hydrochemical characterisation, measurements are carried out in a laboratory at the surface.	Comment understood and accepted.
Measurement errors are not quoted or discussed explicitly for either the laboratory or in situ measurements of formation factor and porosity in the three areas of Sweden described previously. It would have been useful to have an idea of the basic measurement error of the electrical conductivity measurements, although it is understood that these errors are relatively small. (Page 43)	In Forsmark SDM-Site (Crawford, 2008, SKB R-08-48), which is soon to be published, this is done at length.	The more recent report (R-08-48) provides information on measurement errors with supporting discussion (Appendix H).
It is debatable whether the data in Liu et al. (2006) are "*well described by a log normal distribution with mean and standard deviation σ in ^{e}log space*". (Page 45)	From a site descriptive point of view it can be questioned whether the obtained formation factor actually are log-normally distributed. It should have been phrased differently, that the log-normal distribution sufficiently well described the formation factor distribution from a safety assessment point of view. However, measurements from the very homogenous rock mass of rock domain RFM029 in Forsmark show formation factors that are well described by the log-normal distribution	Comment understood and accepted; supported by additional results provided in R-08-48.

	(Crawford, 2008, SKB R-08-48).	
It seems somewhat inconsistent to present all data for formation factors and porosities using lognormal distributions, yet provide recommendations based on the arithmetic mean. (Page 46)	This is done in Liu et al., 2006 based on a reason concerning flowpath averaging. In the SR-Can Data report the same conclusion was made as in SKI 2008:17 and this recommended arithmetic values were disregarded and instead the delivered distributions were used. The motivation was the following: "*In /Liu et al. 2006/ an attempt to average the porosity and formation factor along a flow path is made. However, to avoid the risk that the delivered flow path averaged distributions will be averaged once more in the subsequent modelling, this step has been disregarded by the SR-Can team.*" /SKB TR-06-25, page 193/	Comment understood and accepted.
The value quoted for the diffusivity of iodide in free water, which is in error – it should be $2.0\bullet10^{-9}$ m^2 s^{-1} rather than $0.83\bullet10^{-9}$ m^2 s^{-1}. The value “0.83” has been carried through as far as the Data Report (SKB, 2006b; Table A-40). (Page 46)	Error in SKB-documents.	OK
The typical spacing is cited in SKB (2006b; p. 193) as 10 m, which would appear to suggest a value of 5 m for the central and maximum values. However, a value of 10 m is then cited in the former report (SKB, 2006b; p. 194). (Page 47)	The maximum penetration depth should be half the spacing, i.e. 5 m. Error in the Data report.	OK
With regard to recommendations on porosity in SR-Can, the central values are a factor of 5 less than the previous recommendations. (Page 48)	One cannot directly compare the central value in a log-normal space (SR-Can) and arithmetic space (SR-97). The porosity is rather about 2.5 times lower in SR-Can.	Comment understood and accepted. It was not clear that an arithmetic mean was used in SR-97. Also, there was some confusion on the part of the reviewer between the recommendations for PA on porosity made by Liu et al. compared with those in the SR-Can Data Report.
Examination of the data recommendations provided in Liu et al. (2006) and accepted by the SR-Can team, indicate that the key difference in terms of sensitivity is the reduction in recommended porosity, by a factor of 5. Given that the SR-Can team also retains a factor of 10 reduction in porosity	This is not true. The porosity is smaller in SR-Can (giving less storage capacity for non-sorbing ions). Furthermore the formation factor is about the same as in SR97 or 10 times less (in case of anions) giving similar or reduced capacity for retention by matrix diffusion. The intention of the reviewer appears to have been that D_a of non-sorbing species	Comments understood and accepted. The ‘reduction factor of 10 in porosity for anions’ was a misreading of the text in the SR-Can Data Report. However, lower porosity also means greater penetration into

for anions from SR97, this means that the extent of matrix diffusion will be greater than in the previous assessment. (Page 49)	is increased in SR-Can as the porosity is decreased. This would seemingly give an increased retention due to matrix diffusion. However, in the MPG-group that is of great importance for retention, the effective diffusivity, and not the apparent diffusivity, is included. It should be underlined that for anions the factor 10 reduction is recommended for the formation factor but not for the porosity.	the rock matrix by non-sorbing radionuclides, the extent of penetration presumably being dependent on the maximum penetration depth adopted in the modelling calculations.
Given that measurements of porosity are carried out only in the laboratory, an argument could be made for using a combination of laboratory formation factor and porosity measurements to generate the required diffusion coefficients, primarily in the interests of self-consistency. This is not a criticism of the in situ measurements of formation factors, but rather a desire for a self-consistent dataset. (Page 49)	Within the site investigation/site descriptions, attempts have been made to estimate the in situ porosity by means of estimating the fraction of the laboratory porosity that has been induced by sample preparation and de-stressing. This is done both by a new method of measuring the porosity and by mechanical isostatic load measurements. If feasible, it would be preferable to deliver sets of formation factors and porosities that should both represent in-situ conditions (which would be a self-consistent dataset).	Comment understood and accepted.
SR-Can has highlighted Ra-226 as the most potent radionuclide to pose a risk. Has SKB investigated the sorption properties in terms of Kd of Ra-226 in the site investigations? (Page 52)	Such measurements have been performed on samples both from Forsmark and Laxemar. Preliminary results indicate that the measurements have delivered reasonable results. Data are in line with those of SR-97 but indicate that those used in SR-Can are too high (Crawford, 2008, SKB R-08-48).	We understand that laboratory sorption experiments using site-specific rock samples are ongoing, and that more relevant sorption data for Ra-226 will be available for SR-SITE.
While the general trend in specific surface area as a function of volumetric mean grain size is reasonable, an interesting feature from Figure 13 is that the specific surface areas of Swedish rock types analysed is about a factor of 5-10 lower than those of Finnish rocks, for which a substantial number of sorption data were selected. This observation suggests that for the few elements for which the bulk of data was used as a basis for K_d estimation are from Finland, an extra ‘correction’ factor is needed. (Page 52)	The Finnish samples appear to have been prepared in such a way that a range of grain sizes has been used. The value marked in Figure 13 (in SKI 2008:17) represents the largest fraction in the range. Likely the BET area is much influenced by the fraction of the smaller grains in the sample. If studying Figure 13 and assuming that the Finnish dots at the larger value (2 mm) represent a range between either 0-2 mm or 0.1-2 mm, the values correspond better to the Swedish values.	Comment understood. Given the perceived unspecified range in grain size of the Finnish data, it is probably not appropriate to include them in such a plot.

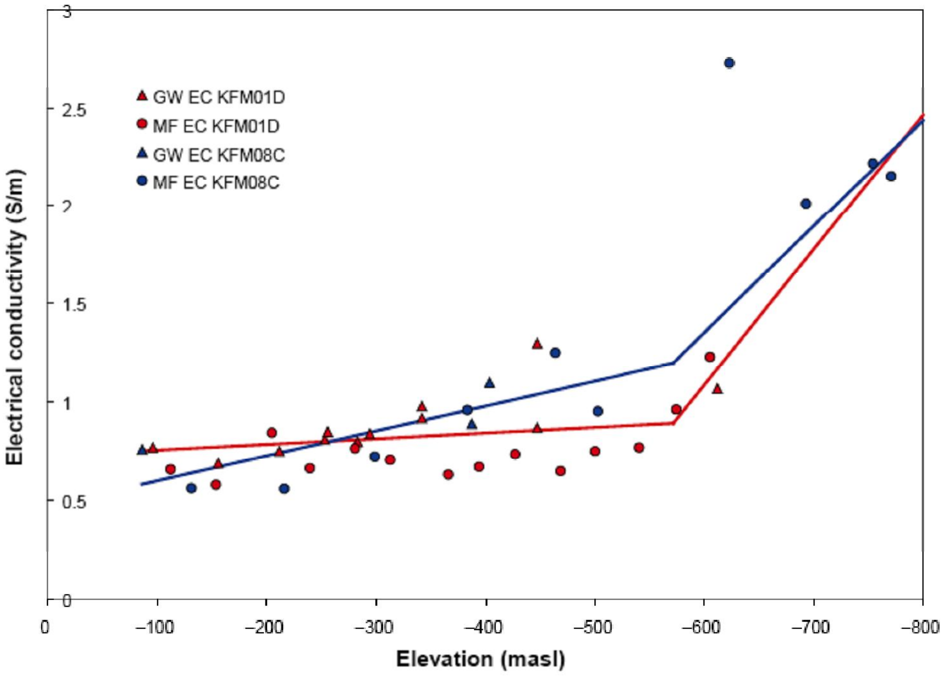

Figure 13: Groundwater and pore water electrical conductivity (EC) at *in situ* temperature in boreholes KFM01D and KFM08C (from Löfgren, 2007, SKB P-07-138).

9. Summary

The following conclusions from the 2008 Workshop and discussions among SKB and its consultants, and SSM and its consultants, are presented as bullet points:

- SSM's consultants agreed that SKB's treatment of uncertainty had improved significantly since its previous assessment, SR-97. However, additional improvements were still possible and recommended, particularly in the area of error propagation according to internationally-approved methods. (This comment is the motivation for Section 6 on uncertainty assessment).

- With regard to the instant release fraction for the spent fuel source term, while a robust model exists for quantifying this release fraction, improvements are needed to decrease the current uncertainty and associated conservatism – measurement on fresh fuels; assess the evolution of grain boundaries – can they open with time?

- With regard to the matrix, radiolytic dissolution is expected to be a significant early process, but the activity threshold needs to be assessed better. For PA, the hydrogen influence on radiolysis may be of second order – the redox buffer capacity of the environment may sufficiently hinder the radiolysis. Solubility-controlled dissolution needs to be studied, in particular, the influence of the U(IV) secondary phases.

- While SSM's consultants generally agreed that SKB's treatment of spent fuel dissolution, in particular matrix alteration, was probably conservative, there was a need for an overall understanding of the underlying mechanism(s). At the very least, a combination of experimental work and mechanistic model development was considered important in terms of increasing confidence in effective parameters and utilised safety assessment treatment, and international consensus for a suitable model would also help greatly.

- The methodology used by SKB for the selection of both elements and their respective species is unclear. Although it may be based on expert judgement this is neither stated explicitly nor is it appropriate. The apparent exclusion of data will undoubtedly lead to increased uncertainty with respect to the concentration limits assigned. For example, it is not clear why SKB was selective in choosing the major ions to be included in the model. The exclusion of Mg and K may have a considerable impact on the magnitude of the free anion concentrations (in particular, sulphate) since these cations are important in at least one of the modelled groundwater scenarios.

- With regard to the determination of solubility limits, uncertainties in the thermodynamic database uncertainty and error propagation were addressed to some extent but not yet in what SSM's consultants believed to be a state-of-the-art manner. In addition, the lack of Pu(III) phosphate data was not addressed. While SSM's consultants agreed that phosphate data for actinides were generally not reliable, SKB needs a strategy to deal with phosphate and the lack of reliable data. On a similar theme, thermodynamic data for Th(IV) needed to be updated, while no satisfactory justification was provided on the use of analogues for specific actinides.

- From the discussions during the Workshop, it was clear that SKB had answers to many of the questions that had been posed previously, e.g., in the area of the thermodynamic database. The problem is that arguments are not explicitly given to justify the data selection in the thermodynamic database. Other questions posed in the reviewer's 2008 report (Stenhouse et al., 2008) have not yet been explicitly addressed by SKB.

- SSM's consultants noted an apparent disconnect or lack of coordination between SKB's experts in the sense that knowledge/information was not being shared to an extent sufficient to address and resolve deficiencies / discrepancies in various SKB reports. This observation was based on the fact that SKB experts at the Workshop were able to provide satisfactory responses to many of the questions raised, e.g., justification of certain data, but these experts were not necessarily part of the team(s) responsible for the areas of interest in which those questions were asked. As one specific example, the omission of Pu(IV) colloid data was justified within the Workshop discussion yet not addressed within SKB's presentations or documentation.

- Triangular distributions often featured in SKB reports and in this context, a number of key issues cause some reservations regarding their use in favour of the Normal distribution. As discussed in Section 7, such reservations include the lack of emphasis on the distribution tails compared with the Normal distribution, the complexity of error propagation compared with the relatively simple method for combining the standard deviations of two Normal distributions, and Monte Carlo sampling and the associated output in terms of the extreme values of an MC sample, which will always be narrower than the extremes of the original triangular distribution. Thus, if a distribution other than the Normal distribution is to be preferred to describe variance and variability, a solid understanding of the properties of the chosen alternative distribution is necessary. This leads to a number of additional concerns / questions, identified at the end of Section 7.

- With regard to radionuclide migration in the far-field, it is clear that SKB and its consultants are at the forefront in terms of measurement technologies applied to the geosphere. However, broader application of, for example, electrical methods to determine appropriate parameters for matrix diffusion combined with additional peer-reviewed publications will help to increase confidence in this area.

- With regard to far-field sorption data, SKB's ongoing experimental programme to generate site-specific sorption data, particularly for the key (dose-limiting) radionuclide) Ra-226, will increase the relevance of, and confidence in, parameter values input to assessment calculations.

References

Andersson, M., Ervanne, H., Glaus, M.A., Holgersson, S., Karttunen, P., Laine, H., Lothenbach, B., Puigdomenech, I., Schwyn, B., Snellman, M., Ueda, H.8, Vuorio, M., Wieland, E. and Yamamoto, T. (2008) Development of Methodology for Evaluation of Long-term Safety Aspects of Organic Cement Paste Components, Joint Working Report by SKB / Posiva / NUMO / NAGRA, Posiva Working Report No. 2008-28.

Aldrich, J. (1997) R.A. Fisher and the Method of Maximum Likelihood 1912-1922, *Stat. Sci.* **12**, 162.

Baas-Becking, L.G.M., Kaplan, I.R. and D. Moore, D. (1960) Limits of the Natural Environment in Terms of pH and Oxidation-Reduction Potentials. *J. Geol.* **68**, 243.

Bath, A. (2008) Abbreviated hydrochemistry database "*rev4_16.11.06.xls*".

Bath, A. and Hermansson, H.-P. (2006) Variability and Uncertainties of Key Hydrochemical Parameters for SKB Sites, SKI Technical Report 2007:03.

Beckman, R.J. and Cook, R.D. (1983) Outlier…..s, *Technometrics* **25**, 119.

Crawford, J. (2006) Data and assessment uncertainty for radionuclide Kd partioning coefficients in granitic rock for use in SR-Can calculations, SKB Technical Report R-06-75, Swedish Nuclear Fuel and Waste Management Company, Stockholm.

Delakowitz, B. (1989) Grundwasseranalytik. Report RCM 00689, Technical University München, Germany, 110 pp.

Duro, L., Grivé, M., Cera, E., Gaona, X., Domènech, C.and J Bruno, J. (2006a) Determination and assessment of the concentration limits to be used in SR-Can, SKB Technical Report TR-06-32, Swedish Nuclear Fuel and Waste Management Company, Stockholm.

Duro, L., Grivé, M., Cera, E., Domènech, C. and Bruno, J. (2006b) Update of a thermodynamic database for radionuclides to assist solubility limits calculation for performance assessment. SKB Technical Report TR-06-17, Swedish Nuclear Fuel and Waste Management Company, Stockholm, 2006b.

EURACHEM/CITAC (2000) *Quantifying Uncertainty in Analytical Measurement*. At http://www.measurementuncertainty.org.

EURACHEM/CITAC (2002) *Traceability in Chemical Measurement*. At http://www. measurementuncertainty.org.

Ekberg C, Meinrath G. and Strömberg B. (2003) A retraceable method to assess uncertainties in solubility estimations exemplified by a few Americium solids. *J. Chem. Thermodynamics* **35**: 55–66.

Fisher, R.A. (1970) Statistical Methods for Research Workers,14th edition, Oliver & Boyd London, U.K., 362 pp.

Fisher, R.A. (1935) *The Design of Experiments*, First Edition, Oliver & Boyd, Edinburgh, U.K.

Fisher, R.A. (1925) *Statistical Methods for Research Workers*, First Edition, Oliver & Boyd, Edinburgh, U.K.

Gallup, G.H. (1939) *Public Opinion in a Democracy*. Princeton University, Princeton, New Jersey, U.S.A.

Gigerenzer, G. (2004) Mindless statistics, *J. Socio-Econ.* **33**, 587.

Gosset, W. (1908) The probable error of mean, *Biometrika* **6**, 1.

Hald, A. (1998) *A History of Mathematical Statistics from 1750 to 1930*, John Wiley and Sons, New York, New York.

ISO (1993) Guide to the Expression of Uncertainty in Measurement Geneva 1993, 1995.

Jeffree, R.A., Markich, S.J. and Brown, P.L., 1993 Comparative accumulation of alkaline-earth metals by two freshwater mussel species from the Nepean River, Australia: Consistencies and a resolved paradox. *Aust. J. Mar. Freshwater Res*. **44**, 609-634.

Kalin, M., Fyson, A. and Meinrath, G. (2007) Natural hydroxide precipitates: Their acid generation potential in ground water associated with tailings, *Proc. 7th Int. Conf. Acid Rock Drainage* St. Louis, Missouri, U.S.A., p. 885.

Kalin, M., Fyson, A. and Meinrath, G. (2006) Observations on the Groundwater Chemistry in and below a Pyretic Tailings Pile and Microbiology, *Proc. 9th Int. Mine Water Congress*, Oviedo, Spain, p. 29.

Kendall, M.G. (1942) Annals of Eugenics **11**, 300.

Lau, P.C.K., Bergeron, H. and Kalin, K. (2001) Bacterial consortia in a ground water plume from acid generating tailings. *Proc. 4th Int. Symp. Waste Processes and Recycling in Mineral and Metallurgical Industries*, MET SOC, Toronto, p. 371.

Liu, J., Löfgren, M. and Neretnieks, I. (2006) SR-Can - Data and uncertainty assessment: Matrix diffusivity and porosity in situ. SKB Report R-06-111, December 2006. Swedish Nuclear Fuel and Waste Management Co., Stockholm, Sweden.

Meer, P., Mintz, D., Rosenfeld, A. and Kim, D. (1991) Robust regression methods in computer vision - a review. *Int. J. Computer Vision* **6**, 59.

Meinrath, G. (2008) Letter to the Editor, *Accred. Qual. Assur.* **31**, 331.

Meinrath, G. and Schneider, P. (2007) *Quality Assurance in Chemistry and Environmental Science*. Springer Heidelberg, Germany, 342 pp.

Meinrath, G., Camoes, M.F., Spitzer, P., Bühler, H., Mariassy, M., Pratt, K. and Rivier, C. (2007) Traceability of pH in a metrological context, in: (Fajgelj, Belli, and Sansone, eds.) *Combining and Reporting Analytical Results*, Royal Society of Chemistry Publications London, U.K., p. 85.

Meinrath, G., Volke, P., Helling, C., Dudel, E.G. and Merkel, B.J. (1999) Determination and interpretation of environmental water samples contaminated by uranium mining activities. *Fresenius J. Anal. Chem.* **364**, 191.

Ochs, M. and Talerico, C. (2004) Data and uncertainty assessment: Migration parameters for the bentonite buffer in the KBS-3 concept, SKB Technical Report TR-04-18, Swedish Nuclear Fuel and Waste Management Co., Stockholm, Sweden.

Pipon, Y., Bererd, N., Moncoffre, N., Peaucelle, C., Toulhoat, N., Jaffrezic, H., Raimbault, L., Sainsot, P. and Carlot, G. (2007) Chlorine diffusion in uranium dioxide under heavy ion radiation, Nuclear Instruments & Methods in Physics Research. B, Beam Interactions with Materials and Atoms vol.257.

Poinssot, C. and 22 coauthors (2005b Final Report of the European Project "Spent Fuel Stability under Repository Conditions", FIKW-CT-2001-00192 SFS. Edited by C. Poinssot & C. Ferry, Report CEA-R-6090, Commissariat à l'Énergie Atomique, Saclay, 104 pp.

Rousseeuw, P.J. and van Drissen, K. (1999) A fast algorithm for the minimum covariance maximum determinant estimator, *Technometrics* **41**, 212.

Rousseeuw, P.J. (1997) Introduction to positive breakdown methods, in: (Maddala and Rao eds.) *Handbook of Statistics* Vol. 15 Elsevier Amsterdam, Netherlands, p. 101.

Rousseeuw, P.J. (1993) A resampling design for computing high-breakdown regression. *Stat. Prob. Letters* **18**, 125.

Saidy, M., Hocking, W.H., Mouris, J.F., Garcia, P., Carlot, G. and Pasquet, B. (2007) Thermal diffusion of iodine in UO_2 and UO_{2+x}, J. Nuclear Materials, vol. 372 (2-3), 405-415.

Salsburg, S. (1985) The religion of statistics as practised by medical journals. *Am. Stat.* **39**, 220.

Schmidt, R. (1934) Statistical analysis of one-dimensional distributions, *Annals of Mathematical Statistics* **5**, pp. 30–43.

Selroos, J-O. (2008) Responses to questions posed in SKI 2007:18, SKB document 2008-06-11, Swedish Spent Fuel and Waste Management Company, Stockholm.

SKB (2006a) Long-term safety for KBS-3 repositories at Forsmark and Laxemar - a first evaluation, Main report of the SR-Can project, SKB Technical Report TR-06-09, Swedish Spent Fuel and Waste Management Company, Stockholm.

SKB (2006b) Data report for the safety assessment SR-Can. SKB Report Technical Report TR-06-25. Swedish Nuclear Fuel and Waste Management Co., Stockholm, Sweden.

SKB (2006c) Fuel and canister process report for the safety assessment SR-Can, SKB Technical Report TR-06-22, Swedish Spent Fuel and Waste Management Company, Stockholm.

SKB (2006d) Buffer and backfill process report for the safety assessment SR-Can, SKB Technical Report TR-06-18, Swedish Spent Fuel and Waste Management Company, Stockholm.

SKB (2006e) Geosphere process report for the safety assessment SR-Can, SKB Technical Report TR-06-19, Swedish Spent Fuel and Waste Management Company, Stockholm.

SKI (2007) Spent Fuel Dissolution and Source Term Modelling in Safety Assessment, Report of Workshop, Sigtuna, Sweden, May 17-19, 2006, SKI Report 2007:17, Swedish Nuclear Power Inspectorate, Stockholm, Sweden.

Stenhouse, M; Brown, P; Ekberg, C; Jégou, C; Meinrath, G; Nitsche, H. (2008) Review of SR-Can: Evaluation of SKB's handling of spent fuel performance, radionuclide chemistry and geosphere transport parameters, SKI report 08:17, Swedish Nuclear Power Inspectorate, Stockholm.

Werme, L.O., Johnson, L.H., Oversby, V.M., King, F., Spahiu, K., Grambov, B. and Shoesmith, D.W. (2004) Spent fuel performance under repository conditions: A model for use in SR-Can, SKB Technical Report TR-04-19, Swedish Nuclear Fuel and Waste Management Company, Stockholm.

Appendix A: The Role of Microbiological Systems in Natural Aqueous Environments

Groundwater analysis is an important part of site characterisation for nuclear waste repositories. A wide variety of groundwaters may be observed in a geological formation depending on, for instance, its history, permeability and recharge characteristics. Groundwater chemistry is affected by inorganic, organic and biological processes all of which may differ even at a fine scale. Dissolution and precipitation, as well as sorption and desorption, affect groundwater composition. Under these circumstances, groundwaters may be expected to vary widely in their physico-chemical properties, and they do in some cases.

The sampling and analysis of groundwaters in the formations above the Gorleben salt dome in Germany yielded groundwaters with sodium chloride concentrations ranging from drinking water quality to saturated NaCl brines and with organic content (mostly fulvic and humic substances) from clear to dark brown (Delakowitz, 1989). Nevertheless, the range of key properties of these waters, e.g. pH, E_H and carbonate content of these groundwaters were found to fall within a well-defined range in agreement with general observation on groundwaters (Baas-Becking et al., 1960).

Baas-Becking et al. (1960) observed that living systems control the aqueous systems and associated the observed limits of natural environments with the redox boundaries established by bacterial processes as shown in Figure A-1. From the observation of near coincidence of the observed boundaries [of natural aqueous environments] with the redox conditions established by relevant bacterial consortia, Baas-Becking et al. concluded:

> "*it appears that the E_H-pH limits of biological systems and of the natural occurring aqueous environment almost coincide. This would indicate that there are few, if any, sterile terrestrial environments caused by limiting E_H-pH characteristics*".

Figure A-2 shows the results of a study concerning the remediation of a mine waste management area in northern Ontario (Kalin et al., 2006, 2007) using ecological engineering techniques. Subsurface water samples were collected and analysed, including microbial isolation and analysis (Lau et al., 2001). The observed E_H and pH data of all groundwaters sampled closely coincided with the limits associated with iron bacteria. Genetic analysis of the isolated bacteria indicated the predominance of iron-reducing species.

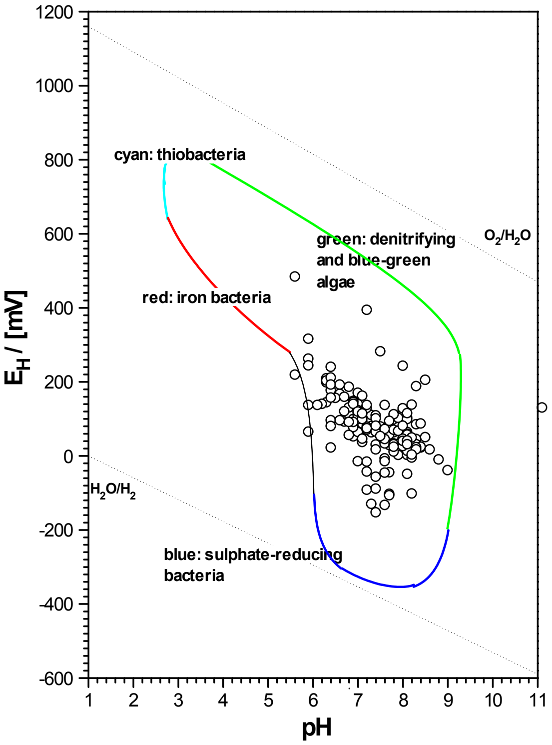

Figure A-1: Limits of the natural environments in terms of oxidation-reduction potentials (E_H) and pH as obtained from about 6200 data pairs on waters with a wide variety of conditions and origins (Baas-Becking et al., 1960). The coloured boundaries give the microbiological processes limiting E_H/pH of natural aqueous systems. The circles give the location of 170 E_H/pH values measured for groundwaters in the formations above the Gorleben salt dome.

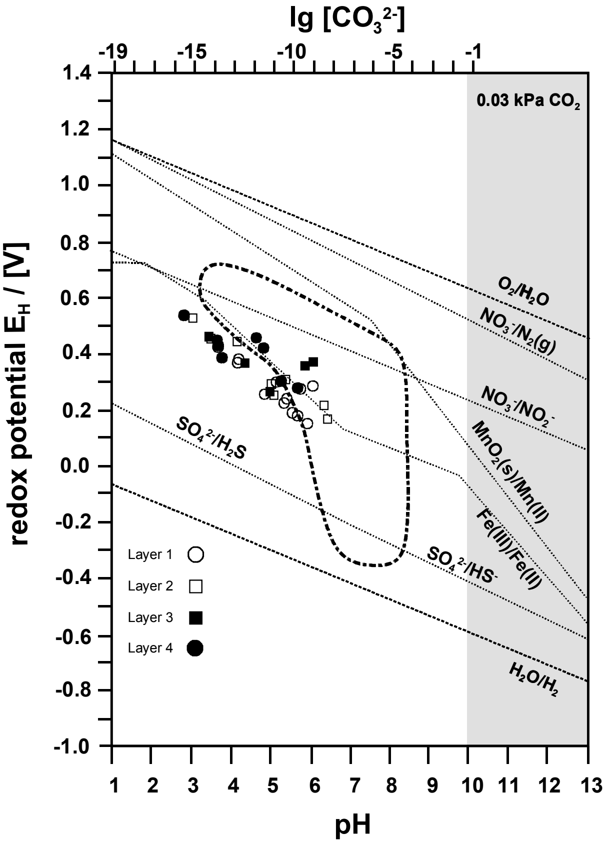

Figure A-2: Limits of the natural environments (boomerang-shaped area) and relevant inorganic redox processes (dashed lines) are given together with field data (Kalin et al., 2006) on oxidation-reduction potentials (see legend).

<u>Note</u>: The grey-shaded region on the right side of the diagram is physically not accessible because the ionic strength *I* would exceed the limit of I = 0.1.

Annex A: Swedish groundwater data (Bath, 2008)

The four tables below contain the data used from the spreadsheet file "*Abbreviated hydrochemistry database rev4_16-11-06.xls"* provided for Swedish groundwaters (Bath, 2008). The Excel sheet is complemented by SKI report 2007:03 "*Variability and Uncertainties of Key Hydrochemical Parameters for SKB Sites*" (Bath and Hermansson, 2006), which describes in detail various relationships and properties within the Swedish groundwater data. While Figures in the report provide several E_H-pH diagrams calculated for various groundwater constituents under the modelled conditions for selected site data, the report does not contain a visual summary of the observations. The E_H-pH relationships displayed in this report (Section 4) are aimed at improving an understanding / interpretation of the data.

Table A1: Forsmark groundwater data.

pH	**E_H** (mV)	**lg [HCO_3^-]** lg (mol dm^{-3})	**Site**
7.47	-195	-3E0	KFM01A/115
7.6	-188	-2.7897E0	KFM01A/180
7.99	--	-2.2078E0	KFM02A/59
7.52	-225	-2.2376E0	KFM02A/116
7.37	--	-2.8168E0	KFM02A/423
7.18	-143	-2.6884E0	KFM02A/512
7.3	--	-2.781E0	KFM03A/388
7.49	--	-2.8263E0	KFM03A/450
7.42	-176	-2.8168E0	KFM03A/452
7.55	-196	-3.4429E0	KFM03A/642
7.78	-245	-3.8311E0	KFM03A/943
8.26	-130	-4.0072E0	KFM03A/990
7.16	--	-2.7439E0	KFM04A/234-inclined
7.27	100	-2.8932E0	KFM04A/357-inclined
--	-274	--	KFM05A-inclined at 55.4d
7.41	-155	-3.1041E0	KFM06A/357-inclined
8.26	-200	-4.0072E0	KFM06A/771-inclined
8	9	-4.0072E0	KFM07A/925-inclined

Table A2: Laxemar groundwater data.

pH	**E_H** (mV)	**lg [HCO_3^-]** lg (mol dm^{-3})	**Site**
8.1	--	-2.8662	KLX01/274
8.2	--	-2.8932	KLX01/458
8.1	--	-3.4051	KLX01/691
7.6	--	-3.4051	KLX01/691
8.1	--	-4.0072	KLX01/835
8.4	--	-4.0072	KLX01/915
8.4	--	--	KLX01/915
8.2	--	-3.7062	KLX01/1038
7.8	--	-2.437	KLX02/318
8.2	-100	-2.4821	KLX02/337
7.6	-40	-2.74	KLX02/800
7.9	-120	-2.4489	KLX02/800
8.5	-125	-3.8822	KLX02/1093
7.6	-170	-3.7062	KLX02/1160
7.9	--	-3.8311	KLX02/1350
--	--	--	KLX02/1389
6.4	-400	--	KLX02/1560
7.9	-300	-3.8311	KLX02/1560
8.58	--	-2.2526	KLX03/35
8.46	--	-2.2388	KLX03/56
8.18	--	-2.3524	KLX03/160
--	-275	--	KLX03/412
8.27	--	-2.3082	KLX03/548
--	--	--	KLX03/647
6.89	--	-3.1725	KLX03/726
7.73	--	-2.2748	KLX04/107
8.12	--	-2.2829	KLX04/158
8.63	--	-2.3428	KLX04/269
--	--	--	KLX04/366
--	--	--	KLX04/458
7.83	--	-3.0778	KLX04/513
--	--	--	KLX04/657
--	--	--	KLX04/774
--	--	--	KLX04/921
7.61	--	-3.8822	KLX04/974

Table A3: Simpevarp groundwater data.

pH	**E_H** (mV)	**lg [HCO_3^-]** lg (mol dm^{-3})	**Site**
7.36	-220	-3.3874	KSH01A/161
7.34	-210	-3.5549	KSH01A/253
7.97	-230	-3.7853	KSH01A/556
7.97	-230	-3.7853	KSH01A/556
7.63	-230	-3.7439	KSH01A/556
8	-230	-3.7853	KSH01A/556
8	-230	-3.7853	KSH01A/556
7.94	--	-2.4449	KSH02/116
7.47	--	-2.6151	KSH02/216
6.83	--	-4.0864	KSH02/421
--	--	--	KSH02/423
8.13	--	-4.0072	KSH02/577
7.72	--	-2.4051	KSH03A/50

Table A4: Äspö groundwater data.

pH	**E_H** (mV)	**lg [HCO_3^-]** lg (mol dm^{-3})	**Site**
7.5	-257	-2.9341	KAS02/208
7.73	-308	-3.7853	KAS02/532
8.5	-150	-3.7439	KAS02/892
8	-275	-3	KAS03/131
8	-275	-3.7439	KAS03/931
--	-275	-2.9465	KAS04/338
8.1	-280	-3.4631	KAS04/460

Appendix B: Good Laboratory Practice (GLP) and Guide to the Expression of Uncertainty in Measurement (GUM)

B.1 Introduction

Assessment of uncertainty is an essential element of scientific data determination. Without a reasonable estimate of the doubt associated with a measured value of a quantity the value itself is meaningless. As a direct consequence of the early 1960's Food and Drug Administration associated with thalidomide and the subsequent Kennedy Hearings of the U.S. Congress, Good Laboratory Practice (GLP) was introduced, the internationally accepted definition of GLP being:

> "*Good Laboratory Practice (GLP) embodies a set of principles that provides a framework within which laboratory studies are planned, performed, monitored, recorded, reported and archived. These studies are undertaken to generate data by which the hazards and risks to users, consumers and third parties, including the environment, can be assessed for pharmaceuticals (only preclinical studies), agrochemicals, cosmetics, food additives, feed additives and contaminants, novel foods, biocides, detergents etc…..GLP helps assure regulatory authorities that the data submitted are a true reflection of the results obtained during the study and can therefore be relied upon when making risk/safety assessments*".

GLP focuses mainly on consumer good quality and OECD promotes GLP on an international basis. Data reliability is a key issue as stated in the last sentence of the above definition and, not surprisingly is also a key issue in the performance assessment of nuclear waste repositories.

During implementation of GLP the lack of an internationally agreed convention on the evaluation of data uncertainty became apparent. Hence the figures appearing occasionally after the value of a physical quantity, e.g., d = 55 ± 3 have in most cases an undefined significance and cannot be compared. Thus, OECD addressed the BIPM (Bureau International des Poids et Mésures, Sèvres). A working group was established in 1976 coming forward with Recommendation INC-1 in 1980 by a panel of international experts in metrology. INC-1 eventually led to the issue of the 'Guide to the Expression of Uncertainty in Measurement" (GUM) by seven international bodies: BIPM, IUPAC, IUPAP, OIML, ISO, IEC and IFCC. Since 1993, therefore, an international consensus on the expression of uncertainty in measurement exists.

Before the introduction of the GUM a laboratory issuing data on the basis of experimental measurements faced three tasks: a) extensive explanations had to be given on the measurement uncertainty calculations; b) keeping random and systematic uncertainties separate even though both were uncertainties; and c) balancing the quest for conservatism with the need to have small overall uncertainties, e.g. in hypothesis testing. The GUM was intended to overcome these tasks.

B.2 Procedure

The international consensus on the expression of uncertainty is based on a four-step procedure:

<u>Step 1</u>: *Create a model of the measurement*
If a model with many uncertainty components becomes complicated, it will usually be possible to subdivide the model into smaller parts. The smaller parts can then be analysed separately.

<u>Step 2</u>: *Identify and characterise each uncertainty component*
The GUM suggests preparing a table containing all uncertainty components. Furthermore, a cause-and-effects diagram (occasionally named 'Ishikawa diagram' according to its inventor) may be produced where the relationship among the uncertainty components can easily be visualised.

<u>Step 3</u>: *Calculate the values of the standard uncertainties u*
Calculating the uncertainty components requires some understanding of standard statistics. Since it is reasonable to assume (at least for simple cases) that a result is affected by many contributing factors, the Central Limit Theorem provides a theoretical basis for expecting a Normal distribution. Thus the individual uncertainty components may be combined using the rules of error propagation. For adding uncertainty components u_i, the following formula is appropriate:

$$u_{comb} = \sqrt{\sum_{i=1}^{N} (u_i)^2}$$

The number of experiments should be large to assume that a Normal distribution applies. If the number of experiments is below 30, the resulting distribution is not Normal but Student *t*. Furthermore, if the number of experiments varies in the different steps of an experimental study, the Welch-

Satterthwaite formula is suggested for the evaluation of effective degrees of freedom ν_{eff}.

$$\nu_{eff} = \frac{u_{comb}^4}{\sum_{k=1}^{N} \left[\frac{(c_i u_i)^4}{\nu_i} \right]}$$

where c_i accounts for Student's t for ν_i degrees of freedom in the assessment of the *i*-th uncertainty contribution. A basic working knowledge in statistics is certainly required in dealing with measurement uncertainty.

<u>Step 4</u>: State the final result

The result of a measurement value for quantity Q should be given as "$Q = (X \pm y)$ units", with a statement that y has been evaluated as u_{comb} according to the GUM and 'units' gives the physical units of the measured quantity. The GUM suggests stating the expanded uncertainty U as $U = k\, u_{comb}$ with an appropriate expansion factor k to represent 95 % coverage. If the degrees of freedom ν_{eff} are above 20, $k = 2$ is acceptable.

Over the past 15 years of its existence the GUM procedures have found widespread application. The GUM has been addressed with substantial criticism as is to be expected for a document with far-reaching influences.

Part of the criticism addresses the complexity of the GUM often referring to the extensive use of statistical nomenclature and partial derivatives. In particular, those fields where neither statistics nor mathematics (or both as in chemistry) is an essential part of the academic curricular education, experience difficulties in familiarization with the GUM rules. For chemistry, EURACHEM has issued several supporting guides, e.g. "*Quantifying Uncertainty in Analytical Measurement*" and "*Traceability in Chemical Measurement*". The current modernisation of the GUM will introduce Monte Carlo approaches to uncertainty estimation partly responding to the enormous increase in micro-processing speeds since the original GUM made its way into the scientific community.

The assessment of measurement uncertainty according to an international consensus is not a new concept but has existed for a long time. The problem has always been how to unify uncertainty reports to make them comparable.

Annex B: Extracts from “*Development of Methodology for Evaluation of Long-term Safety Aspects of Organic Cement Paste Components*” by Andersson et al., (2008)

The following (italicised) text is taken from a section of the draft report dealing with batch sorption experiments. For clarity, a few changes have been made to the text, and those changes are included within square brackets.

“To begin with the deduction of an experimental equation for the R_d coefficients[3]*, it should be noted that these are usually expressed in the unit m^3/kg. This is because the solid is usually measured by its mass m and not by its volume, and also because of the experimental limitation where the amount of adsorbed material is measured indirectly, by measuring what is left in solution and using the mass balance, the volume of solution V must also be included.*

R_d values are therefore commonly given as:

$$R_d(m^3/kg) = \frac{A_{ads} \cdot V}{A_{aq} \cdot m} \qquad \text{(eq.4-7)}$$

Note that A_{ads} *is expressed here as mol adsorbed on solid per volume of solution.*

Since the experiments must be carried out in a container (in this case centrifugation tubes), there is always a second solid phase present: the container wall. There is consequently a need for a supporting [parallel] *experiment, a reference, where only wall sorption is measured.*

An alternative way to measure wall adsorption…………..is to break off the experiment at the desired sampling time, empty the tubes, refill with acid and then measure what the acid desorbs from the walls.

Both methods have their risks for introducing errors, possible flaws with the method of a [parallel wall sorption] *experiment will soon be shown.*

---

[3] R_d = experimental measurement of the distribution coefficient, K_d.

Applying the expression for R_d on a supporting experiment, without solid, gives:

$$R_{d,ref} = \frac{A_{wall,ref} \cdot V_{ref}}{A_{aq,ref} \cdot m_{wall}} \qquad \text{(eq.4-8)}$$

A terminology is now introduced with R_d, without further indexing, as the corresponding coefficient for the batch sorption experiment with solid added to the tubes, $R_{d,ref}$ as the coefficient for a batch sorption experiment without added solid and finally $R_{d,g}$ *as the coefficient for the solid, (g =granite). Henceforth,* [the index] w *will be used for wall.*

In order to obtain $R_{d,g}$, which is of primary interest here, the mass balances for each tube must be used

$$A_{tot} = A_{aq} + A_g + A_w + \sum_{i=1}^{n-1} A_{utt,i} \qquad \text{(eq.4-9)}$$

$$A_{tot,ref} = A_{aq,ref} + A_{w,ref} + \sum_{i=1}^{n-1} A_{utt,i,ref} \qquad \text{(eq.4-10)}$$

The summation terms, with indexes utt, i, are to compensate for the n-1 samples taken [prior to] *the sampling occasion* n.

The total amounts A_{tot} and $A_{tot,ref}$ *have to be measured separately. In this work a separate tube is used, where the stock tracer solution has been added to 1M HCl to ensure zero wall sorption. Samples from this are then taken and measured at the same time as samples from the other tubes. Actually, one sample of this acidic reference would suffice, but the reasoning for taking further samples was that a mean value of several samples would give a more exact value of the total amount added. The samples could have been taken anytime, but were conveniently taken at the same time when the other samples were taken (one day, one week and one, three and six months).*

The concentration C of tracer in the acidic reference is therefore a mean value

$$\overline{C} = \frac{1}{n} \sum_{1}^{n} \frac{A_{utt,i,sur}}{V_{utt,i,sur}} \qquad \text{(eq.4-11)}$$

$A_{utt,i,sur}$ and $V_{utt,i,sur}$ *are the measured tracer activity and sampling volume for the acidic reference at sampling occasion* i, *respectively.*

Using the mean concentration of tracer stock solution in the mass balances yields

$$\overline{C} \cdot V_{stam} = A_{aq} + A_g + A_w + \sum_{i=1}^{n-1} A_{utt,i} \qquad \text{(eq.4-12)}$$

$$\overline{C}\cdot V_{stam,ref} = A_{aq,ref} + A_{w,ref} + \sum_{i=1}^{n-1} A_{utt,i,ref} \qquad (eq.4\text{-}13)$$

Here V_{stam} and $V_{stam,ref}$ *are the volumes of tracer added to tubes with and without solid, respectively.*

$R_{d,ref}$ can now be expressed as:

$$R_{d,ref} = \frac{\left(\overline{C}\cdot V_{stam,ref} - A_{aq,ref} - \sum_{i=1}^{n-1} A_{utt,i,ref}\right)\cdot\left(V_{0,ref} - \sum_{i=1}^{n-1} V_{utt,i,ref}\right)}{A_{aq,ref}\cdot m_w} \qquad (eq.4\text{-}14)$$

Here the volume of the reference sample at the start, $V_{0,ref}$, is adjusted for previous samplings.

It is desirable to express $A_{aq,ref}$ in quantities that are actually measured. The relation is:

$$A_{aq,ref} = \frac{A_{utt,n,ref}\cdot\left(V_{0,ref} - \sum_{i=1}^{n-1} V_{utt,i,ref}\right)}{V_{utt,n,ref}} \qquad (eq.4\text{-}15)$$

Inserting this in the expression for $R_{d,ref}$ yields:

$$R_{d,ref} = \left(\frac{\overline{C}\cdot V_{stam,ref}\cdot V_{utt,n,ref}}{A_{utt,n,ref}} - V_{0,ref} + \sum_{i=1}^{n-1} V_{utt,i,ref} - \frac{V_{utt,n,ref}\cdot\sum_{i=1}^{n-1} A_{utt,i,ref}}{A_{utt,n,ref}}\right)\cdot\frac{1}{m_w} \qquad (eq.4\text{-}16)$$

Since the mass of the tube wall participating in sorption, m_w, is unknown, instead of $R_{d,ref}$, it is necessary to measure the quantity

$$R_{d,ref}\cdot m_w \qquad (eq.4\text{-}17)$$

Note that this quantity for measuring sorption onto the tube wall is a volume and has the unit m^3 (or mL in the results presented here). Replicate experiments for wall sorption are made here, so again, a mean value can be utilised

$$\overline{R_{d,ref}\cdot m_w} \equiv L_d \qquad (eq.4\text{-}18)$$

For a shorter notation the label L_d has been introduced; there is no convention for this, so any label can do.

A crucial point now emerges: can this L_d be utilised for measuring sorption on tube walls in the tubes with solid added? A development of $R_{d,ref}$ gives:

$$R_{d,ref} = \left(\frac{K_{d,A} + K_{d,AOH} \cdot [OH] \cdot \beta_{AOH} + K_{d,AOH_2} \cdot [OH]^2 \cdot \beta_{AOH_2} + ...K_{d,AL} \cdot [L] \cdot \beta_L}{1 + [OH] \cdot \beta_{AOH} + [OH]^2 \cdot \beta_{AOH_2} + ...[L] \cdot \beta_L} \right) \cdot \frac{V_{ref}}{m_w}$$

(eq.4-19)

Note that K_d constants for wall sorption of each solution species appear in the numerator.

This shows that $R_{d,ref}$ is constant, as long as:

1) [OH] is constant, and

2) Free organic ligand concentration, [L], is constant.

So, when utilising separate experiments for tube wall sorption, it must be assured that the pH is exactly the same in the experiments with and without solid and that the added solid does not affect the free concentration of L.

The first requirement is made here by initially adjusting pH in both tubes to the same value. The second requirement is simply assumed: sorption of L onto the added solid is negligible compared to what is left in solution. However, separate measurements of L sorption onto granite are also made here (see Results section……..), which have verified this assumption: the sorption of superplasticisers onto granite is very weak.

With precautions taken and warnings made, it is possible to utilise $R_{d,ref}$ in the form of L_d in the mass balance for the sample with solid phase, to [obtain]*:*

$$\overline{C} \cdot V_{stam} = A_{aq} + \frac{L_d \cdot A_{aq}}{V_0 - \sum_{i=1}^{n-1} V_{utt,i}} + A_g + \sum_{i=1}^{n-1} A_{utt,i} \qquad \text{(eq.4-20)}$$

After some algebra, solving for $R_{d,g}$ from this, the result is:

$$R_{d,g} = \left(\frac{\overline{C} \cdot V_{stam} \cdot \left(V_0 - \sum_{i=1}^{n-1} V_{utt,i} \right)}{A_{aq}} - \left(V_0 - \sum_{i=1}^{n-1} V_{utt,i} \right) - L_d - \frac{\left(V_0 - \sum_{i=1}^{n-1} V_{utt,i} \right) \cdot \sum_{i=1}^{n-1} A_{utt,i}}{A_{aq}} \right) \cdot \frac{1}{m}$$

(eq.4-21)

Again, in order to express A_{aq} in what is actually measured, the relation needed is:

$$A_{aq} = \frac{A_{utt,n} \cdot \left(V_0 - \sum_{i=1}^{n-1} V_{utt,i} \right)}{V_{utt,n}} \quad \text{(eq.4-22)}$$

Utilising this, the equation for $R_{d,g}$ is, finally:

$$R_{d,g} = \left(\frac{\overline{C} \cdot V_{stam} \cdot V_{utt,n}}{A_{utt,n}} - \left(V_0 - \sum_{i=1}^{n-1} V_{utt,i} \right) - L_d - \frac{V_{utt,n} \cdot \sum_{i=1}^{n-1} A_{utt,i}}{A_{utt,n}} \right) \cdot \frac{1}{m}$$

(eq.4-23)

Note that the terms inside the brackets are all volumes. It is also fairly simple to compare the terms for importance and unreasonable values, for example, such as those that would yield negative $R_{d,g}$.

4.1.2 Random error propagation in batch sorption measurements

Since only random and uncorrelated errors caused by fluctuations in measurements are considered here, this section is an exercise in the application of the error propagation formula on a function F(x,y...)

$$\sigma_F^{\ 2} = \sigma_x^{\ 2} \cdot \left(\frac{\partial F}{\partial x} \right)^2 + \sigma_y^{\ 2} \cdot \left(\frac{\partial F}{\partial y} \right)^2 + \ldots.. \quad \text{(eq. 4-24)}$$

The function F(x,y...) to apply the formula on is $R_{d,g}$ [eq.4-23]. Since L_d and C, the parameters for wall sorption and concentration of the acidic reference, respectively, are used as mean values, the measured standard deviations of the replicates are taken as errors for these parameters.

Furthermore, the relative errors in the measured volumes and solid mass are judged to be small in comparison, since they were weighed with a laboratory balance.

Therefore, weighing errors were not considered, only errors in number of counts of the radioactive tracer for $A_{utt,n}$*, the last sampling, and* $A_{utt,i}$*, the previous samplings were considered, together with the standard deviations for* L_d *and C.*

The error in $\mathrm{R}_{\mathrm{d,g}}$ *is therefore calculated as:*

$$\sigma_{Rd,g} = \frac{1}{m} \cdot \sqrt{\sigma_C{}^2 \cdot \left(\frac{V_{stam} \cdot V_{utt,n}}{A_{utt,n}} \right)^2 + \sigma_{A_{utt,n}}{}^2 \cdot \left(\frac{V_{utt,n}}{A_{utt,n}{}^2} \cdot \left(\sum_{i=1}^{n-1} A_{utt,i} - C \cdot V_{stam} \right) \right)^2 + \sigma_{L_d}{}^2 + \left(\frac{V_{utt,n}}{A_{utt,n}} \right)^2 \cdot \sum_{i=1}^{n-1} \sigma_{A_{utt,i}}{}^2}$$

(eq.4-25)

By analysing the results, it was found that the last two terms were insignificant compared with the first two terms and they can safely be omitted in the calculation of the error for $R_{d,g}$*."*

Appendix C: Properties of the Triangular Distribution

C.1 Introduction

The discussion here focuses on the properties of the triangular distribution and its use as an alternative to the Normal distribution of interpreting experimental data[4].

The Normal distribution is characterised by just two parameters: the mean μ, and the standard deviation, σ. The probability of an event, ξ, is thus given as

$$p(\xi) = \frac{1}{\sigma\sqrt{2\pi}}\exp(-\frac{(\xi-\mu)^2}{2\sigma^2}.$$

The parameters μ and σ were termed 'statistics' by Fisher, the person primarily responsible for developing and expanding the application of statistics during the 1920’s to 1950’s (Kendall, 1942).

Choosing a Normal distribution to interpret experimental data is not simply the selection of one method among many. Rather, the Normal distribution provides an unparalleled insight into data analysis, based on a solid foundation provided by a number of mathematicians including de Moivre, Gauss, and Laplace (Hald, 1998). In particular, Laplace’s Central Limit Theorem (CLT) shows that the Normal distribution is the large-sample limit of a number of other distributions such as the Poisson and the χ^2 (chi square) distributions. Lindeberg and Lévy independently identified a series of conditions (now called the Lindeberg-Lévy conditions) under which the CLT is valid and Hoeffding subsequently provided a formal proof that, if a distribution is part of a class of distributions named ‘U statistics’, then the Lindeberg-Lévy conditions are valid and the validity of the CLT is warranted.

Careful analysis of data, especially experimental data, is needed to justify an alternative approach to the Normal distribution, given the latter’s widespread use and long-term experience and application. One possible reason for an alternative approach may be small sample size. Thus, because many well-known statistics, e.g. the standard deviation and the mean, are Normally distributed only in the case of a large sample size, it is important to apply the correct distribution when dealing with small samples. Gosset (1908) discusses where the limit between ‘small’ and ‘large’ sample size should be drawn. Subsequently, Fisher (1970) provided a formal proof of Gosset's

---

[4] "*Statistics is the branch of scientific method which deals with the data obtained by counting or measuring the properties of populations of natural phenomena*”, Sir Maurice G. Kendall.

derivation. Ignoring small sample statistics may result in considerable bias in statistical inference (Meinrath, 2008).

Modern terminology more often refers to the mean value and the standard deviation as ‘estimators’ rather than ‘statistics’. If, for instance, μ and σ have been obtained for a set of experimental data, together they describe everything that can be concluded about the experiment. In many situations, however, multiple candidates can act as estimators of the parameters μ or σ, e.g., the mean or median as an estimator for μ. Fisher (1970) proposed several criteria for a good estimator:

- Consistency: The more data that are available the greater the probability that the calculated estimator is close to the true value of the parameter.
- Lack of bias: After using a particular estimator many times on different sets of data, the average of the values of the estimator should come close to the true value of the parameter.
- Efficiency: Although values of the estimator will not be exactly equal to the true value of the parameter, most of the estimators of a parameter should not be too far from the true value.
- Sufficiency: Alternative estimators may exist but will not provide any additional information about a parameter from the same sample.

As an illustrative example, Figure C-1 shows the results of a round robin study on pH together with its interpretation by its closest-fitting cumulative Normal distribution. The probability that the results are distributed normally and that deviations are the result of random sampling is > 90 %. This figure indicates that the Normal distribution is not just an arbitrarily-selected probability distribution. Rather, the Normal distribution, together with other distribution functions of the class of U statistics which approach the Normal distribution with increasing sample size, are essential components of natural processes, e.g., Maxwell's kinetic theory of gases.

Thus, while data analysis and the application of probability have a solid mathematical foundation, the average scientist / engineer is rarely exposed to this foundation and associated relationships (Salzberg, 1985; Gigerenzer, 2004). There is an increasing tendency for statistical inference to be introduced with recipe-like algorithms, and this situation is further aggravated by the increasing use of statistics software by untrained data analysts.

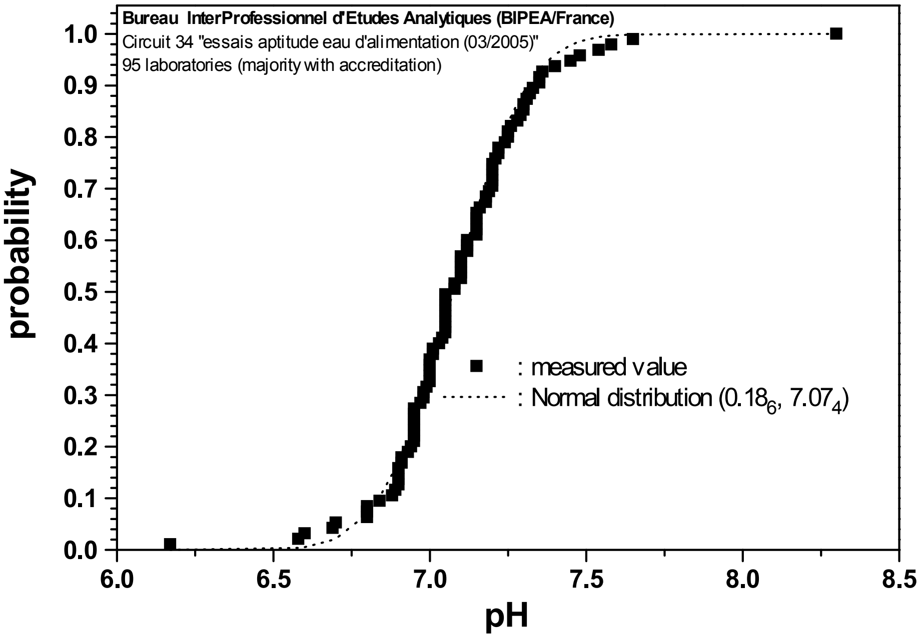

Figure C-1: Measurement of pH in drinking water by 95 laboratories participating in a proficiency testing exercise coordinated by Bipea, France. The reported mean value results are given as an empirical probability distribution and interpreted by its closest-fitting cumulative Normal distribution with a standard deviation of 0.18 pH units (Meinrath et al., 2007).

C.2 Characteristics of Triangular Distribution

The triangular distribution is characterised by three parameters:

1) Minimum value, d_u;
2) Maximum value, d_o;
3) Mode, m.

The mode gives the location of the maximum probability density. Thus, the standard symmetric triangular distribution with $d_u = 0$, $d_o = 1$ and $m = 0.5$ is defined by the probability density function (see Figure C-2):

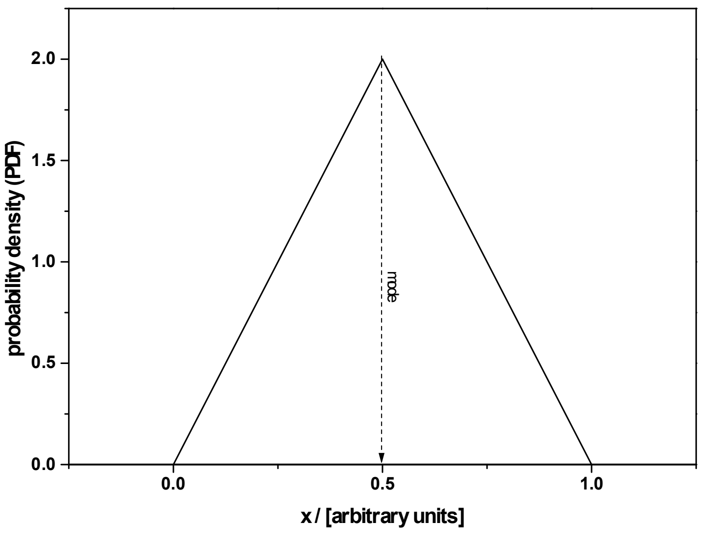

Figure C-2: Standard symmetric triangular distribution with support[5] [0,1].

$$p(x) = \begin{cases} 4x, & for\; 0 < x \le \frac{1}{2} \\ 4(1-x) & for\; \frac{1}{2} \le x \le 1 \\ 0 & elsewhere \end{cases}$$

The expectation E of the triangular distribution is the mean m_t:

$$m_t = \frac{d_u + d_o + m}{3},$$

while the standard deviation s_t is given by

$$s_t = \sqrt{\frac{d_u^2 + d_o^2 + m^2 - d_u m - d_o m - d_u d_o}{18}}$$

The literature concerning the triangular distribution is sparse between 1757, when Simpson applied it to combination-type gaming problems and 1934, when Schmidt realized that the standard symmetric triangular distribution is the mathematical combination of two standardized uniform distributions (Schmidt, 1934). Schmidt's finding also provides a convenient way of generating random triangular deviates by setting

$$p_{tri} = \frac{rnd_1 + rnd_2}{2}$$

---

[5] The support of a distribution is the smallest closed interval/set whose complement has probability zero.

where rnd_1 and rnd_2 are random numbers drawn from independent uniform distributions with support [0,1].

Figure C-3 shows a comparison of the standard triangular distribution in [0,1] together with its closest-fitting Normal distribution. The probability that the samples collected from a triangular distribution is in fact obtained from a Normal distribution and that the observed differences are due to random effects is almost always >95 %. Thus, comparing the hypothesis H_1: "*The difference between data sampled from a symmetric triangular distribution and from a Normal distribution can be distinguished*" with the Null hypothesis: "*The respective differences just appear as being from random effects*" will result in the statement: "*The Null hypothesis can be rejected in less than 5% of cases"*. From a series of simulation experiments performed within this study the conclusion had to be drawn that this result may be independent of sample size. Given this outcome, it is difficult to understand why the benefits of the Normal distribution (in particular the solid theoretical principle of reasoning, e.g., on the basis of maximum likelihood theory), are sacrificed in favour of an unusual distribution which has been investigated to a significantly lesser extent.

Figure C-3 shows the differences between the probability densities of a symmetric triangular distribution and Normal distribution. The triangular distribution has specified maximum and minimum values. Because the area below the probability density distribution is unity by definition, the location of the extreme values d_u and d_o has a very sensitive influence on the overall distribution. On the other hand, the Normal distribution is unbounded, and accounts for observations a long way from the expected value (usually the mean). Experimentalists are familiar with such observations, which often occur with a higher frequency than is consistent with the Normal distribution. Such observations are termed 'outliers' or 'discrepant observations'. Outliers are not accounted for in triangular distributions.

Both distributions describe essentially the same shape in the vicinity of the expected value. The Normal distribution emphasizes the central tendency while the symmetric triangular distribution emphasizes the mid range section. In this range (up to about *2s* or 2 standard deviation in terms of the Normal distribution) the probability densities are rather close indicating that any symmetric triangular distribution can be closely modelled as a Normal distribution.

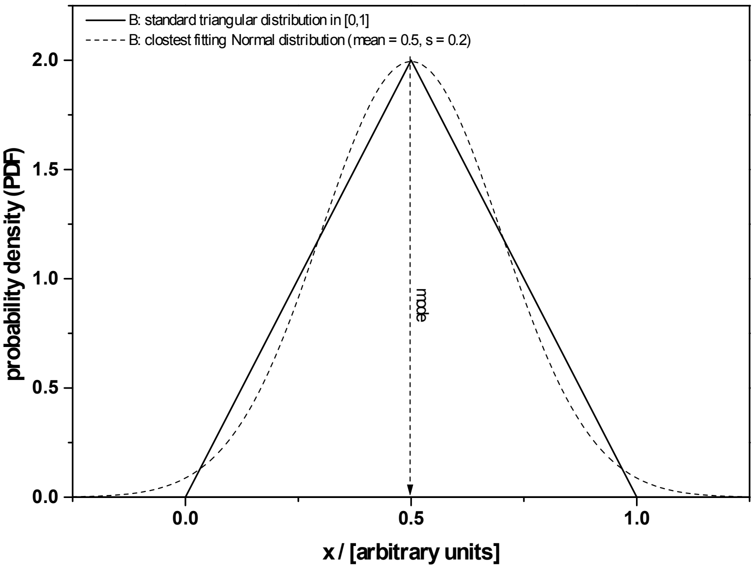

Figure C-3: Comparison of a standard triangular distribution with support [0,1] with its closest-fitting Normal distribution. The probability (on the basis of a sample size of 2000 random numbers obtained from the triangular distribution) that the triangular distribution is in fact Normal and observed differences are due to random effects is >0.95.

In contrast to the Normal distribution, the triangular distribution does not need to be symmetric. The extreme situation is a triangular distribution where the mode *m* is equal to either d_u or d_o. For an asymmetric triangular distribution, the mode *m* is no longer equidistant between d_u and d_o. The density function is defined by the probability density function

$$p(x) = \begin{cases} \dfrac{2(x-d_u)}{(d_o-d_u)(m-d_u)}, & \text{for } d_u \le x \le m \\ \dfrac{2(d_o-x)}{(d_o-d_u)(d_o-m)} & \text{for } m \le x \le d_o \\ 0 \quad \text{elsewhere} & \end{cases}$$

There is nothing like an 'standard asymmetric triangular distribution', because the shape of the distribution will vary with *m*. However, any asymmetric triangular distribution can be transformed into a standard symmetric distribution, using the above definition. The denominators in the above definition of the asymmetric triangular distribution assure that the area under the probability density is unity, and these denominators depend on *m*. The numerators consist of straight-line functions of *x*. Thus the CDFs are derived readily, *viz.*

$$CDF(x) = \begin{cases} \dfrac{(x-d_u)^2}{(d_o-d_u)(m-d_u)}, & \text{for } d_u \le x \le m \\ 1-\dfrac{(d_o-x)^2}{(d_o-d_u)(d_o-m)} & \text{for } m \le x \le d_o \end{cases}$$

The distribution becomes simplified if m equals either d_u or d_o, in which case one of the terms in the above mathematical definition disappears.

Two representative asymmetric triangular distributions are shown in Figure C-4a, both with support [2,5]. In one case, the dashed arrow gives the location of the mode for the distribution with $m = 3$. In the other case, the mode m is equal to d_o. The corresponding cumulative distributions are shown in Figure C-4b. In the case of the triangular distribution the mode is not necessarily (at least asymptotically) equal to the mean. Similarly, the median and mean may converge to different values even in the case of a large sample limit, which differs significantly from the Normal distribution. Knowing either the mean or the median provides no information about the location of the mode. The mode, however, is essential in obtaining the shape of an asymmetric triangular distribution from a set of data.

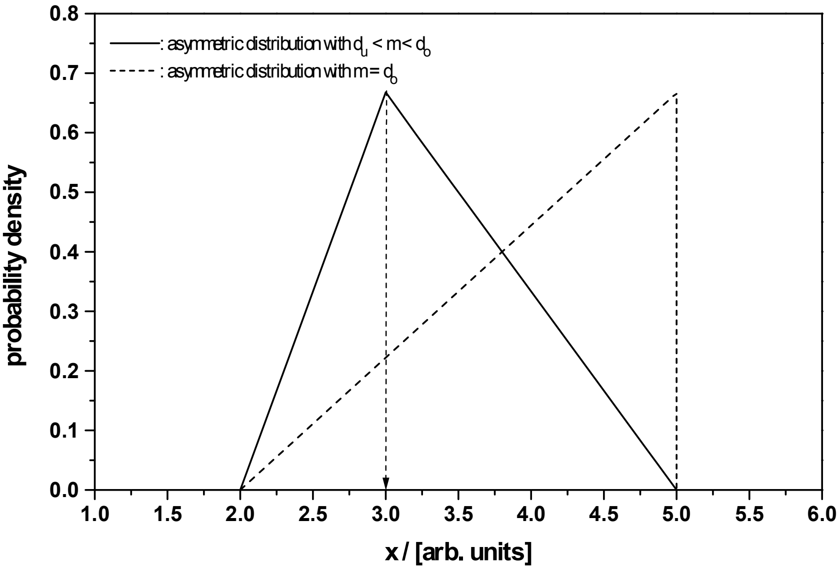

Figure C-4a: Probability densities of two triangular distributions with support [2,5]. The solid line represents an asymmetric distribution with a mode $m \neq d_o$, in case of the dashed line $m = d_o$.

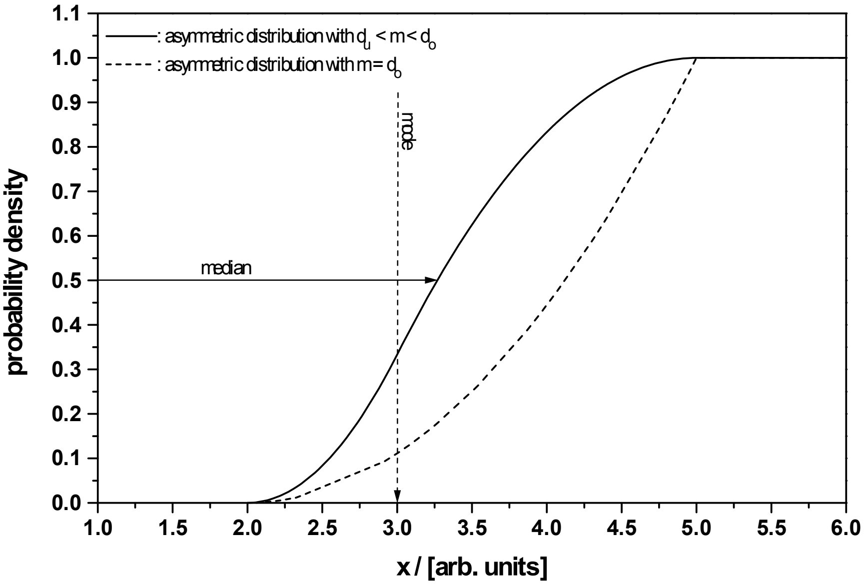

Figure C-4b: Cumulative probability distributions of two triangular distributions with support [2,5]. The solid line represents an asymmetric distribution with mode $m \neq d_o$. In the case of the dashed line, $m = d_o$. Note that the mode is not equal to the median. For the solid line ($m \neq d_o$), i = 3 while the median = 3.24 and the mean = 3.33. For the dashed distribution ($m = d_o$) c = 5 while both the median and mean = 4, while m = 5.

Estimating the mode m from a set of (supposedly) triangularly distributed data requires order statistics and maximum likelihood estimation. Alternatively, Kolmogorov-Smirnov statistics or χ^2 fitting are used to estimate the location of the mode.

C.3 Alternatives to Triangular Distribution

Alternatives to a triangular distribution do exist, e.g., the Weibull distribution, which is a parametric distribution with three parameters, *viz.*

$$w(x) = \frac{c}{a}\left(\frac{x-\mu}{a}\right)^{(c-1)} \exp\left[-\left(\frac{x-\mu}{a}\right)^{c}\right]$$

with $x \geq \mu$ and $a,c > 0$, where a is the scale parameter, c the shape parameter and μ the location parameter. Although the definition of the Weibull distribution may seem complicated, it is close to the definition of the Normal distribution. The term preceding the exponential is a normalisation factor ensuring that the integral over the function $w(x)$ equals unity. The exponential itself may be seen as a generalisation of the exponential known from the Normal distribution where the variable c replaces the constant 2.
An important property of the Weibull distribution is its asymmetry, expressed by the shape parameter. The following graphs refer to the standard

Weibull distribution having μ = 0 and a = 1. The expression of the Weibull functions thus simplifies to:

$$w(x) = c\,x^{c-1}\exp(-x^{c}).$$

Graphical representation of the standard Weibull distribution is given in Figure C-5 for various values of the shape parameter c. Figure C-5 illustrates that the Weibull distribution may represent an asymmetric as well as a symmetric distribution of data. The Weibull distribution cannot interpret data where the mode is skewed to the right-hand side (cf. Fig. C-4a). However, such a case may easily be treated by a suitable transformation of data. A special feature of the Weibull distribution is its similarity to the Normal distribution for c = 3.6. In fact, a power transformation with k = c/3.6 can be applied to non-Normally Weibull-distributed data ***V*** with V^k having approximately Normal distribution. Hence, subjecting asymmetrically-distributed data to a power transformation allows the use of deeply explored and widely applied Normal distribution properties like error progression and confidence limit estimation after an appropriate transformation.

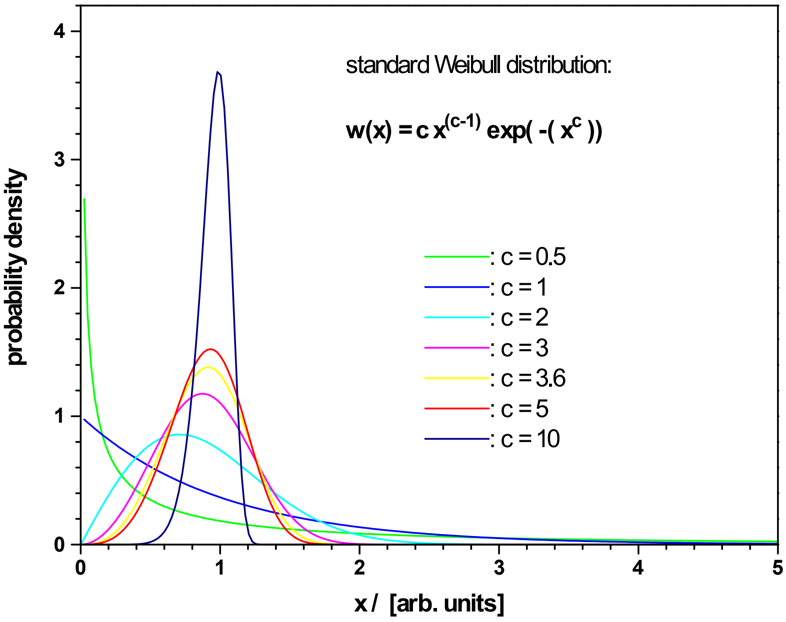

Figure C-5: Plots of the standard Weibull distribution for various shape parameters c.

Strålsäkerhetsmyndigheten
Swedish Radiation Safety Authority

SE-171 16 Stockholm
Solna strandväg 96

Tel: +46 8 799 40 00
Fax: +46 8 799 40 10

E-mail: registrator@ssm.se
Web: stralsakerhetsmyndigheten.se